

THE ROLE OF IBR5 IN REGULATING PLANT AUXIN RESPONSE THROUGH  
THE SCF<sup>TIR1</sup> COMPLEX

by

Timothy J. Cioffi, B.S.

A thesis submitted to the Graduate Council of  
Texas State University in partial fulfillment  
of the requirements for the degree of  
Master of Science  
with a Major in Biology  
May 2019

Committee Members:

Nihal Dharmasiri, Chair

Sunethra Dharmasiri

Hong-Gu Kang

**COPYRIGHT**

by

Timothy J. Cioffi

2019

## **FAIR USE AND AUTHOR'S PERMISSION STATEMENT**

### **Fair Use**

This work is protected by the Copyright Laws of the United States (Public Law 94-553, section 107). Consistent with fair use as defined in the Copyright Laws, brief quotations from this material are allowed with proper acknowledgement. Use of this material for financial gain without the author's express written permission is not allowed.

### **Duplication Permission**

As the copyright holder of this work I, Timothy J. Cioffi, authorize duplication of this work, in whole or in part, for educational or scholarly purposes only.

## **ACKNOWLEDGEMENTS**

I would like to thank my advisor, Dr. Nihal Dharmasiri, for his incredible help in pushing me to reach my goals, Dr. Sunethra Dharmasiri for her thoughtfulness and indispensable advice, and Dr. Hong-Gu Kang for being an earnest and inquisitive mentor. I thank Sasha Alanis for always being there for me, even when times were tough. I must also thank my lab mates Idrees Ahmad and Rohit Katti, and all my friends and family for encouraging me to always do my best and never give up on my goals.

## TABLE OF CONTENTS

	<b>Page</b>
ACKNOWLEDGEMENTS .....	iv
LIST OF FIGURES .....	vi
ABSTRACT.....	viii
CHAPTER	
I.    INTRODUCTION .....	1
II.   MATERIALS AND METHODS.....	9
III.  RESULTS .....	20
IV.  DISCUSSION.....	43
REFERENCES .....	54

## LIST OF FIGURES

Figure	Page
1. Genomic response to auxin in plant cells .....	3
2. <i>ibr5</i> mutation disconnects Aux/IAA degradation from auxin-responsive gene induction.....	5
3. IBR5 interacts with ASK1 <i>in vitro</i> independently of auxin.....	21
4. IBR5-ASK1 interaction was not detected <i>in vivo</i> using Co-IP.....	21
5. ASK1 and CUL1 are degraded <i>in vitro</i> via the 26S proteasome .....	22
6. IBR5 regulates steady state levels of ASK1 and TIR1 .....	24
7. <i>ibr5</i> mutants show no altered response to methyl jasmonic acid.....	24
8. Analysis of <i>TIR1</i> gene expression in <i>ibr5-1</i> mutant and overexpression lines.....	26
9. qPCR analysis of <i>ASK1</i> gene expression in <i>ibr5</i> mutant and overexpression lines.....	26
10. <i>35S:IBR5-Myc</i> is not hypersensitive to auxin.....	27
11. Degradation of TIR1 in <i>ibr5-1</i> and <i>35S:IBR5-Myc</i> .....	27
12. Effects of heat stress on TIR1 protein.....	29
13. GDA stabilizes Aux/IAA proteins irrespective of IBR5 activity .....	30
14. IBR5 is involved in plant responses to heat stress.....	31
15. <i>ibr5</i> mutants exhibit increased Aux/IAA degradation using <i>HS:AXR3NT-GUS</i> reporter line.....	32
16. qPCR analysis of heat shock-inducible <i>HS:AXR3NT-GUS</i> in <i>ibr5</i> mutants.....	33
17. <i>35S:DII-Venus</i> is stabilized in <i>ibr5</i> mutant and <i>35S:IBR5-Myc</i> backgrounds.....	34
18. Confocal Z-stack images show <i>35S:DII-Venus</i> stabilization in <i>ibr5</i> mutants .....	35
19. IBR5 does not interact significantly with Aux/IAA proteins <i>in vitro</i> .....	36
20. 3-week old phenotypes of <i>ibr5, sgt1b-4</i> double mutant lines.....	37
21. <i>ibr5, sgt1b-4</i> double mutant lines have increased resistance to 2,4-D compared to single mutants .....	38

22. <i>ibr5</i> , <i>sgt1b-4</i> double mutant lines have increased resistance to IAA compared to single mutants .....	39
23. <i>ibr5</i> , <i>sgt1b-4</i> double mutant lines have different effects on picloram resistance compared to single mutants .....	40
24. <i>sgt1b-4</i> auxin resistance is rescued by overexpression of TIR1, but not <i>ibr5-1</i> or <i>35S:IBR5-Myc</i> backgrounds .....	42
25. Hypothetical model of IBR5 regulating TIR1/ASK1 subcellular localization via the HSP90-SGT1b chaperone module .....	52

## ABSTRACT

Plant growth and development is a highly regulated process that involves synthesis, cellular transport, and perception of the growth hormone auxin, or indole-3-acetic acid (IAA). Cellular responses to auxin involve the degradation of the Aux/IAA family of repressors through SCF<sup>TIR1/AFBs</sup> complex, which is composed of ASK1, CUL1, RBX1, and the F-box protein TIR1/AFBs, subsequently modulating the expression of auxin-related genes to control growth and development. Previous studies identified IBR5 as a gene involved in the auxin response pathway, as primary root growth of *ibr5* mutants exhibited insensitivity to indole-3-butyric acid (IBA), a precursor to IAA in plants, as well as IAA and other auxin analogues. Additionally, *ibr5* is defective in several other hormone and stress response pathways. Interestingly, Aux/IAAs are rapidly degraded in *ibr5* mutants, which is contrary to other mutant genes identified in the auxin signaling pathway. This research sought to characterize the role of IBR5 in regulating the auxin response pathway through the SCF<sup>TIR1/AFBs</sup> complex. Previous results indicated that SCF<sup>TIR1/AFBs</sup> subunit, ASK1, interacts *in vitro* with IBR5. Results of this research indicate that steady-state levels of ASK1 and TIR1 proteins are elevated in *ibr5* mutant and *35S:IBR5-Myc* overexpression lines. Since SGT1b is also known to regulate TIR1 abundance, the genetic interaction between IBR5 and SGT1b was also analyzed. *ibr5*, *sgt1b* double mutants show increased auxin resistance compared to single mutants, suggesting these proteins act partially independently in auxin response. Additionally, post-translational modifications of TIR1, including those mediated by HSP90-SGT1b chaperone modules, were shown to be unaffected in *ibr5* mutants. Together, the results in this study suggest that IBR5 is not involved with the HSP90-mediated stabilization of TIR1, however future testing may reveal IBR5 to be required for proper HSP90-mediated nuclear localization of TIR1.

## I. INTRODUCTION

Plant growth and development is a continuous process, which organizes a plant's body through cell division, expansion, and differentiation. Being sessile organisms, plants must respond to their changing environments in an efficient manner, which often means altering their development. The plant hormone, auxin, plays an important role in coordinating growth and development by regulating the transcription of growth-related genes, and is required for entrance into the cell cycle (Perot-Rechenman 2010). Cellular response to auxin triggers division and elongation, which facilitates a variety of physiological responses such as phototropism and gravitropism (Friml et al. 2002; Swarup et al. 2005). The auxin pathway has also been shown to be integrated with other plant hormone and signaling pathways, further illustrating its pivotal role in plant development (Woodward and Bartel, 2005).

Auxin, the primary native form being indole-3-acetic acid, or IAA, acts in the cell through genomic and non-genomic pathways to regulate plant growth. In the nucleus, auxin regulates the expression of growth-related gene families: Aux/IAA, SAUR, and GH3 genes (Hagen and Guilfoyle, 2002). A family of transcriptional factors called auxin response factors (ARFs) bind auxin-response elements (AuxREs) found in the promoters of these auxin-responsive gene families, and their activity can modulate gene transcription (Li et al. 2016). The Aux/IAAs are a family of repressors that bind and repress the activities of ARFs, and auxin regulates the degradation of the Aux/IAAs to modulate gene expression. Aux/IAAs are understood to achieve their repressive effect by recruiting the transcriptional co-repressor TOPLESS (TPL) to promoters of genes (Szemenyei, Hannon, and Long 2008). TPL interacts with histone deacetylases (HDAC),

removing acetyl groups from lysine residues on nearby histones, resulting in an increased positive charge, which more tightly condenses negatively charged DNA (Kagale and Rozwadowski, 2011; Oh, et al 2014). TPL behaves similarly as a co-repressor in brassinosteroid and jasmonic acid signaling, R-protein mediated immunity, and floral development pathways to transcriptionally deactivate pathway-specific genes (Oh, et al. 2014; Pauwels et al. 2010; Zhu et al. 2010; Krogan, Hogan, and Long 2012).

The auxin-mediated regulation of Aux/IAs depends upon a ubiquitin-ligase (E3) complex, SCF<sup>TIR1/AFBs</sup> (Gray et al. 1999; Dharmasiri et al. 2005). In the Ubiquitin-Proteasomal Pathway (UPP), E3 enzymes are responsible for substrate recognition and ligation of chains of a small protein called ubiquitin, which triggers subsequent recognition by the 26S proteasome for degradation (Choi et al. 2014). SCF complexes are a family of cullin-RING ubiquitin ligase (CRL) found in all eukaryotes (Skaar, Pagan, and Pagano 2013). SCF complexes consist of core subunits CUL1 and RBX1, which are able to bind with many different substrate recognition modules, consisting of SKP1 and an F-box protein (Petroski and Deshaies 2005). In plants, the SCF<sup>TIR1/AFBs</sup> complex is composed of CUL1, RBX1, ASK1 (or Arabidopsis SKP1-like), and the TIR1/AFBs family (TRANSPORT INHIBITOR RESISTANCE1/AUXIN SIGNALING F-BOX) as F-box proteins (Gray et al. 1999). In the auxin pathway, the F-box protein TIR1 (or related AFB) acts as a coreceptor for auxin with the Aux/IAs (Tan et al. 2007). In the presence of auxin, Aux/IAA repressors bind strongly to TIR1, bringing the Aux/IAs in proximity to the E3 ligase, which allows E2 enzymes to conjugate ubiquitin chains, signaling proteasomal degradation of the repressors (Fig. 1) (Dharmasiri, Dharmasiri, and Estelle 2005; Tan et al. 2007; Ramos et al. 2001).

Importantly, the auxin-mediated degradation of Aux/IAAs is required for proper cell expansion. Gain-of-function mutants of many Aux/IAAs results in cell expansion-related defects (e.g., *iaa1/3/7/17*) (Mockaitis and Estelle 2008). Auxin-induced gene expression results in signaling cascades, which activate plasma membrane proton pumps, leading to the acidification of the apoplast surrounding the plant cell membrane. This acidification activates expansin proteins in the apoplast which can loosen cell wall components, allowing for increased turgor pressure to expand the cell (Spartz et al.

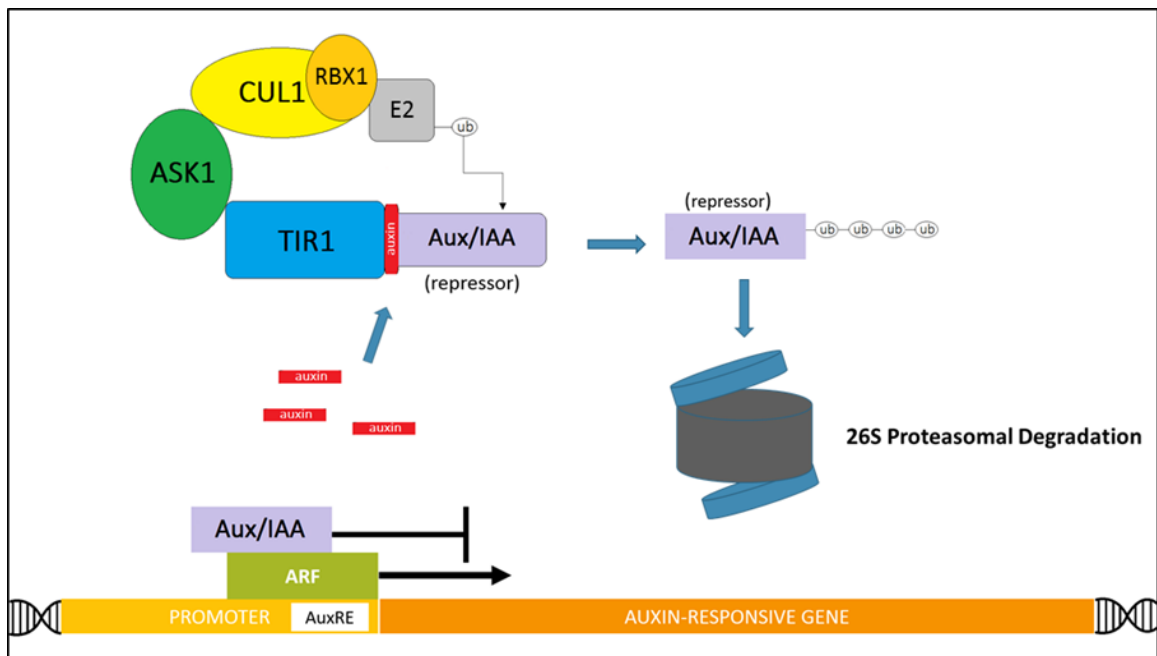


**Figure 1. Genomic response to auxin in plant cells.** ARF transcriptional factors exert their regulatory effects on auxin-responsive genes by binding to the auxin-response elements (AuxREs) located in the promoters of these genes. Aux/IAA repressor proteins bind the ARFs to repress their activity by recruiting co-repressor complexes that condense chromatin. Auxin in plant cells acts as molecular glue between Aux/IAA proteins and TIR1, leading to polyubiquitination of Aux/IAAs, which is a signal for degradation by the 26S proteasome. ARFs are then free to regulate gene expression.

2014). In all cases, auxin-induced gene expression is required for proper plant growth and development.

Traditionally, pieces of the auxin response pathway have been identified and characterized using mutants displaying auxin response-defective phenotypes, often in *Arabidopsis thaliana*. One useful tool is applying exogenous auxins to seedlings at concentrations that are typically inhibitory to root growth and analyzing mutant lines which are resistant to the inhibitory effects. *INDOLE-3-BUTYRIC ACID RESPONSE 5* (*IBR5*) was identified as a gene involved in auxin signaling, as the null mutant *ibr5-1* showed resistance to the inhibitory effects of indole-3-butyric acid (IBA), a natural precursor to IAA (Zolman et al. 2000). In addition, *ibr5-1* was resistant to all natural and synthetic auxins tested, including 2,4-dichlorophenoxyacetic acid (2,4-D) (Monroe-Augustus, Zolman, and Bartel 2003; Strader, Monroe-Augustus, Bartel 2008) and picloram (Jayaweera et al. 2014). Interestingly, while auxin-responsive gene expression is decreased in mutants of *IBR5*, they also exhibit an increased degradation of Aux/IAA repressor proteins. This is contrary to other mutants identified in the auxin pathway, which typically exhibit Aux/IAA stabilization. This suggests that the activity of *IBR5* may mediate Aux/IAA repressor degradation and induction of auxin-responsive genes via a yet unknown mechanism (Fig. 2).

Studies have shown that *IBR5* is involved in multiple hormone signaling pathways including auxin, abscisic acid (Monroe-Augustus, Zolman, and Bartel 2003), and ethylene (Strader, Chen, and Bartel 2010). *IBR5* has also been shown to be important in abiotic stresses such as salt, reactive oxygen species (ROS), and osmotic stress (Jayaweera et al. 2014). Therefore, eliciting the specific function(s) of *IBR5* may shed

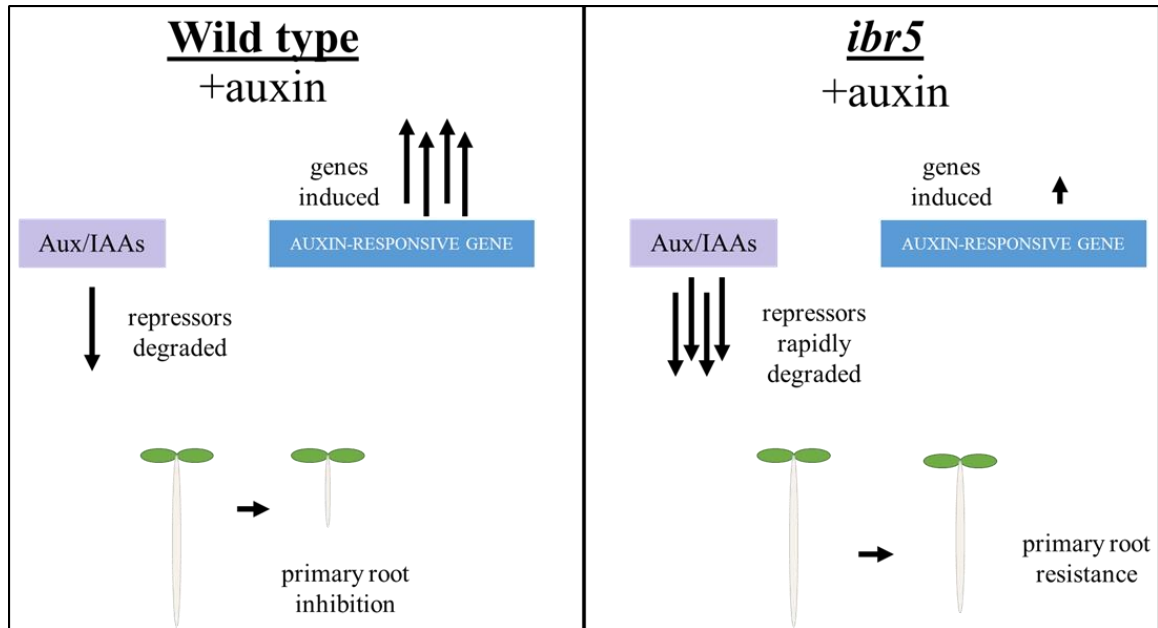


**Figure 2. *ibr5* mutation disconnects Aux/IAA degradation from auxin-responsive gene induction.** In the case of wild type *Arabidopsis*, treatment with exogenous auxin increases Aux/IAA degradation and subsequent auxin-responsive gene induction, and root growth becomes inhibited. In *ibr5* mutants, Aux/IAA proteins are comparatively unstable, yet gene induction is reduced, and root growth is resistant to the inhibitory effects of exogenous auxin. Therefore, IBR5 should connect Aux/IAA degradation with auxin-responsive gene induction.

light on the complex regulation of the auxin pathway via integration with other environmental responses.

IBR5 encodes a dual-specificity phosphatase, and shares ~35% identity with known mitogen-activated protein kinase (MAPK) phosphatases in humans (Monroe-Augustus, Zolman, and Bartel 2003). The phosphatase activity of IBR5 has been tested by many individual groups with varying success, and a MAPK, MPK12, has been identified as an interacting partner for IBR5 (Lee, et al. 2009). MPK12 was recently revealed to play a role in guard cell CO<sub>2</sub> signaling, however IBR5 does not appear to be involved in this process, since the *ibr5-1* displayed no CO<sub>2</sub> signaling defects (Jakobson et al. 2016). Further, MPK12 is mostly expressed in guard cells, while IBR5 is expressed

throughout the plant, particularly in meristematic tissues (Jammes et al. 2009; Monroe-Augustus, Zolman, and Bartel 2003). In contrast, evidence shows the catalytic site of IBR5 is important for its role in auxin signaling. *ibr5-4* is a catalytic site mutant that exhibits auxin resistance similar to *ibr5-1* (Jayaweera et al. 2014). Moreover, overexpressing IBR5 protein with a substitution in the catalytic site only partially complements auxin sensitivity in *ibr5-1*, compared to wild type IBR5 protein. (Strader, Monroe-Augustus, Bartel 2008). Exactly how IBR5 phosphatase activity contributes to auxin signaling remains unknown.

To study the function of IBR5 in auxin signaling, our lab has investigated proteins that interact with IBR5. Using a yeast two-hybrid system, IBR5 was found to interact with several proteins including PAD1, a subunit of the 20S core particle of the 26S proteasome, ARA2, a small GTP-binding protein, and NRPB4, subunit 4 of the RNA polymerase II complex (Kathare, unpublished). In a previous yeast two-hybrid screening aimed at finding ASK protein interactions, the yet unidentified IBR5 was found to interact with ASK1, a subunit of the SCF<sup>TIR1/AFBs</sup> complex (Risseuw et al. 2003). More recently, the Arabidopsis Interactome Mapping Consortium (2011) documented this same interaction in a high-throughput yeast two-hybrid screening, and suggested that ASK1 can be phosphorylated. Given that Aux/IAs are destabilized in *ibr5* mutants, and ASK1 is a core subunit of the SCF<sup>TIR1/AFBs</sup> responsible for triggering Aux/IAA degradation, the characterization of the IBR5-ASK1 interaction may help explain the auxin and stress-related phenotypes observed in *ibr5* mutants and determine the function of IBR5.

Additionally, the interaction between IBR5 and ASK1 proves interesting because IBR5 was shown to form a complex with two proteins, HSP90 and SGT1b, to conduct

holdase activity on R-proteins (Liu et al. 2015). HSP90 is a heat shock protein that acts widely in eukaryotes as a chaperone, regulating protein folding and responses to heat stress (Chen, Zhong, Montiero 2006). *SGT1* was originally identified in *Saccharomyces cerevisiae* as a dosage suppressor of the temperature-sensitive G2 allele of SKP1 (Kitigawa et al. 1999), and researchers demonstrated that SGT1 interacts with SCF complexes containing SKP1 as an essential component for yeast and human kinetochore assembly (Kitigawa et al. 1999; Steensgaard, et al. 2004). It was later found that SGT1 is a co-chaperone for HSP90, acting as a client adaptor for HSP90 to associate with SKP1 (Catlett and Kaplan 2006). In Arabidopsis, SGT1b (homologue of SGT1) was observed to be involved in auxin responses, explained by its interaction with the SKP1 homologue, ASK1, a component of the SCF<sup>TIR1/AFBs</sup> complex (Gray et al. 2003). A recent study showed that inhibiting HSP90, or mutating SGT1b, destabilizes TIR1 protein (Wang et al. 2016). This illustrates that the HSP90-SGT1b interaction with the SCF<sup>TIR1/AFBs</sup> complex regulates the auxin response pathway by modulating the stability of auxin co-receptor, TIR1, (Wang et al. 2016). Additionally, these findings draw a strong connection between heat stress and auxin response (Wang et al. 2016). Given that IBR5 and SGT1b interact and regulate plant disease resistance by stabilizing R-proteins (Liu et al. 2015), and mutations in either protein confer auxin resistance (Zolman et al. 2000; Gray et al. 2003), it would be worth investigating whether these two proteins act together in auxin signaling and heat stress, possibly by regulating the SCF<sup>TIR1/AFBs</sup> complex. Additionally, studying their genetic interactions could help determine if IBR5 and SGT1b contribute to cross-talk between the auxin pathway, heat-stress responses, and R-protein mediated defense responses.

The current study sought to test the hypothesis that the auxin-related effects of IBR5, both physiological and biochemical, are a result of an interaction between IBR5 and ASK1, and indirectly the SCF<sup>TIR1/AFBs</sup> complex. In addition, the study probed the genetic interaction between IBR5 and SGT1b to elicit if these two proteins have related functions in the auxin signaling pathway. Collectively, the findings presented here show that IBR5 regulates the auxin signaling pathway in a manner that is consistent with the modulation of the subcellular localization of components of the SCF<sup>TIR1/AFBs</sup> complex.

## II. MATERIALS AND METHODS

### Plant growth conditions

All *Arabidopsis thaliana* lines used were derived from the *Columbia* (Col-0) ecotype. *ibr5-1* seeds were graciously provided by Dr. Bonnie Bartel, Rice University. *ibr5-4*, *ibr5-5*, and *35S:IBR5-Myc* were previously described (Jayaweera et al. 2014). *sgt1b-4* seeds were provided by Dr. Terence Walsh, Dow AgroSciences. *TIR1:TIR1-HA* (*tir1-1*) and *HS:NT-GUS* seeds were provided by Dr. Mark Estelle, University of California – San Diego. *35S:DII-Venus* seeds were provided by Dr. Teva Vernoux, École Normale Supérieure de Lyon. Potted plants were grown in Pro-Mix BX soil at 22°C under continuous light, unless specified. When seeds were sowed directly onto soil, pots were vernalized for 48 hours before placing in growth room.

Before plating on media, seeds were surface-sterilized using a 40% bleach, 0.04% Triton X-100 solution and washed four times with sterile distilled water, then vernalized at 4°C for 1-2 days. Seeds were plated on sterile *Arabidopsis thaliana* medium with 0.5% sucrose (ATS) containing 0.8% agar. Plates were set vertically in a growth chamber at 22°C under continuous light.

### Generation of double mutants and genotyping

Double mutant lines were generated by manually crossing *sgt1b-4* into *ibr5* mutants, and homozygous lines were confirmed using derived cleaved amplified polymorphic sequence (dCAPS) primers (Table 1). PCR Amplified fragments for *sgt1b-4*, *ibr5-1*, *ibr5-4*, and *ibr5-5* were digested for 2 hours at 37°C using HindIII, SnaBI, BsmAI, and HindIII, respectively, per manufacturer's instructions. Successful digestion

of fragments was assessed by separating bands in a 3% agarose gel at 120V for approximately 1 hour.

To genotype *tir1-1* in *TIR1:TIR1-HA (tir1-1)* lines, a fragment from genomic TIR1 was specifically amplified by using a reverse primer which lies within the 3' untranslated-region of the TIR1 gene, followed by nested PCR to amplify a dCAPS fragment. Nested dCAPS fragments were digested by BsmAI, and digestions were assessed with agarose gel electrophoresis.

Transgenic lines used in this study were genotyped using antibiotic resistances conferred along with the transgenes. Seed populations were sterilized and plated on ATS media containing antibiotics, and segregation of the transgene of interest was based on antibiotic resistance segregation. *35S:IBR5-Myc* and *HS:AXR3NT-GUS* plants were each selected with 50µg/mL kanamycin, *35S:DII-Venus* with 25µg/mL hygromycin, and *TIR1:TIR1-HA* with 50µg/mL glufosinate (phosphinothricin).

### **DNA extraction**

To extract DNA from plant tissues, seedlings or leaf sample were homogenized in 300µL 2X CTAB buffer [2% cetyl trimethylammonium bromide (CTAB) (w/v), 100 mM Tris-Cl (pH 8.0), 1.4 M NaCl, 20 mM EDTA] and heated at 65°C for 30min. 300µL of chloroform was added, and tubes were vortexed well. Tubes were centrifuged at 13,000 x g for 5min, and supernatants recovered into new tubes with 3 volumes of 100% ethanol and placed at -20°C for 30min to precipitate DNA. Samples were then centrifuged at 13,000 x g for 20min at 4°C. DNA pellets were washed with 70% ethanol, centrifuged

again at 10,000 x g for 5min at 4°C, and all ethanol was removed by air drying before resuspending pellets in 10 mM Tris-Cl (pH 8.0). DNA samples were stored at -20°C.

**Table 1. Primer sequences**

Primer	Sequence	Use
sgt1b-4 F	5' GGCCTCCCTTGAATATGGTAAAG 3'	dCAPS
sgt1b-4 R	5' TACACTGGTCTCTGCGAAAGCT 3'	dCAPS
ibr5-1 SnaBI F*	5' GCCTGTTTCTTCCGATACGGTGGCTACG 3'	dCAPS
ibr5 FBOX SalI R**	5' GTAGAGATTCTGGCACATAGG 3'	dCAPS
ibr5-4 F*	5' TCGGTAGTTACGACAACGCTTCTC 3'	dCAPS
ibr5-4 R*	5' ACAACAACCGCTGGTGATCTACTGATA 3'	dCAPS
ibr5-5 F*	5' GTGTTCTTGTGCATTGCATGTCTG 3'	dCAPS
ibr5-5 HindIII R*	5' AAACCTCCTGCAGTTGTTGGTAAAGCT 3'	dCAPS
TIR1 3' R**	5' AATACCCCACCAGGATCTCTCA 3'	Nested PCR
tir1-1 F**	5' GTGCAAGTCATGGTACGAGATCGA 3'	Nested PCR, dCAPS
tir1-1 R**	5' CTCAGGAGATTCACTGAGAGCGAA 3'	dCAPS
qTIR1-HA F	5' AACATGGACCAAGACTCAACAATGA 3'	qPCR, RT-PCR
qTIR1-HA R	5' CATAATCTGGAACATCGTATGGATA 3'	qPCR, RT-PCR
TUA F*	5' GCAGCTATCAGTCCCTGAGATC 3'	RT-PCR
TUA R*	5' TCCACCTTCAGCACCAACTTCT 3'	RT-PCR
qASK1 F	5' GATGACGATCTTAAGGCCTGGGA 3'	qPCR
qASK1 R	5' CAGGTAATTAGCAGCCAGAATGAG 3'	qPCR
qGUS 5' F	5' CCTGTGGGCATTCAGTCTGGAT 3'	qPCR
qGUS 5' R	5' ACTGCCTGGCACAGCAATTG 3'	qPCR
qUBA F*	5' AGTGGAGAGGCTGCAGAAGA 3'	qPCR
qUBA R*	5' CTCGGGTAGCACGAGCTTTA 3'	qPCR
qPP2A F	5' TTAACGTGGCCAAAATGATGCA 3'	qPCR
qPP2A R	5' GTTCTCCACAACCGCTTGGT 3'	qPCR

\* Designed by Sunethra Dharmasiri; \*\* Designed by Thilanka Jayaweera.

## **RNA extraction and cDNA synthesis**

Plant tissue samples for RNA extraction were flash frozen in liquid nitrogen, and ground into a fine powder, which were then added to 1.5mL tubes with 1mL of Tri-Reagent and vortexed well. Homogenates were centrifuged 13,000 x g for 5min at 4°C to remove cell debris. Supernatants were recovered into new tubes with ¼ volume of chloroform, vortexed well, and left at room temperature for 15min. Samples were then centrifuged at 13,000 x g for 10min at 4°C, and the supernatants recovered into new tubes with an equal volume of isopropanol, vortexed well, and left at room temperature for 15min. Samples were then centrifuged at 13,000 x g for 10min at 4°C, and the supernatant discarded. RNA pellets were washed with 70% ethanol, centrifuged again at 8,000 x g for 5min at 4°C, and all ethanol was removed by air drying before resuspending pellets in DEPC-treated water. RNA samples were stored at -80°C.

Before cDNA synthesis, RNA samples were treated with DNase I enzyme (NEB) per manufacturer's instructions to remove any contaminating DNA. Treated RNA samples were then reverse-transcribed into complementary DNA (cDNA) using the M-MuLV RT enzyme (NEB) per manufacturer's instructions. cDNA samples were stored at -80°C, while a 1:50 dilution in Millipore-filtered water was kept at 4°C for as a working solution for RT-PCR and qPCR experiments.

## **qPCR analysis**

Transcript levels of cDNA samples were analyzed by quantitative polymerase chain reaction (qPCR) with SYBR<sup>®</sup> Green using the Bio-Rad CFX Connect Real-Time System according to the manufacturer's instructions. The PCR program was as follows:

55°C for 2min, 95°C for 10min, then 40 cycles of 95°C for 25s and 62°C for 20s. Each sample reaction was carried out in three technical replicates, and the averages were analyzed using the  $\Delta C_T$  method (Livak, Schmittgen 2001). Expression data were normalized against *PP2A* or *UBA* genes and presented as expression relative to these reference genes. All experiments were repeated three times with similar results. Primers used are listed in Table 1.

### **RT-PCR analysis**

cDNA samples prepared from extracted RNA were used as template DNA in PCR reactions to test relative gene expression. Template cDNA concentration was normalized by amplifying the reference gene Tubulin A (*TUA*), and both reference and target genes were amplified at two different cycle numbers to assure equalized bands were not saturated.

### **Protein extraction**

For GST pull-down assays, Co-Immunoprecipitation assays, and *in vitro* degradation assays, seedlings were grown on ATS media for 10-12 days and protein was extracted by homogenizing seedlings in HEPES extraction buffer [50mM HEPES (pH 7.5), 100mM KCl, 10% glycerol (v/v), 0.1% Tween-20 (v/v), 1mM PMSF, 10 $\mu$ M MG132, and protease inhibitor cocktail (Roche)]. For *in vitro* degradation assays, MG132 (26S proteasome inhibitor) was omitted from HEPES buffer. Homogenates were rocked at 4°C for 10min, then centrifuged at 10,000 x g for 10min at 4°C to remove cell debris.

Protein concentrations were estimated and equalized using the Bradford assay (Bradford, 1976).

For western blot analyses, 8-12 seedlings grown on ATS media were homogenized in 1.5mL centrifuge tubes with 1X LSB [Laemmli Sample Buffer: 125mM Tris-Cl (pH 6.8), 2% SDS (w/v), 10% glycerol (v/v), 5%  $\beta$ -mercaptoethanol (v/v)] using small plastic pestles. Homogenates were boiled for 5min before centrifuging at 13,000 x g for 10min to remove cell debris. When root and shoot tissues were extracted separately, seedlings were cut with small scissors approximately 1mm below the root-shoot junction. 40-50 roots and 12 shoots were used per protein sample.

### **GST pull-down assay**

An *Escherichia coli* strain harboring a plasmid with the inducible GST-ASK1 transgene was kindly provided by Dr. William Gray. GST and GST-tagged proteins were expressed in *E. coli* by growing cultures in liquid Lysogeny Broth (LB) containing 100 $\mu$ g/mL carbenicillin at 37°C until reaching an optical density of approximately 0.6 (OD600), followed by treatment with 2mM IPTG for 4-5hrs at 30°C. Pelleted bacterial cells were resuspended in PBS [phosphate buffered saline (pH 7.4): 137 mM NaCl, 2.7 mM KCl, 10 mM NaH<sub>2</sub>PO<sub>4</sub>, 2 mM KH<sub>2</sub>PO<sub>4</sub>], and lysed by sonification. Lysates were supplemented with 1mM PMSF and 0.1% Tween-20 (v/v), and rocked at 4°C for 10min before centrifuging at 10,000 x g at 4°C for 10min to remove cell debris. Supernatants were then incubated with glutathione-agarose beads overnight while rocking at 4°C to purify GST-tagged proteins. Beads were washed three times with PBS + 0.1% Tween-20

for 5min each, and all wash liquid removed by pipetting with a fine-point tip. Washed beads were suspended in PBS and stored at 4°C up to one week before use.

To perform pull-down assays, 600-1000µg total protein from *35S:IBR5-Myc* seedling extract was incubated with 10µL of glutathione-agarose beads previously bound with GST or GST-tagged recombinant proteins microcentrifuge tubes, gently rocking at 4°C for 2hrs. Tubes were then centrifuged at 2,000 x g for 1min, and all protein extract removed. Beads were washed three times with HEPES wash buffer [50mM HEPES (pH 7.5), 100mM KCl, 10% glycerol (v/v), 0.1% Tween-20 (v/v)] for 5min each, and finally resuspended in 15µL 2X Laemmli Sample Buffer (2X LSB) [100mM Tris-Cl (pH 6.8), 4% SDS (w/v), 20% Glycerol (v/v), 10% β-mercaptoethanol (v/v), 0.1% Bromophenol blue (w/v)]. Samples were boiled for 5min and spun-down before loading onto SDS-PAGE gels.

### **Co-Immunoprecipitation assay**

Protein concentrations were estimated and equalized using the Bradford assay (Bradford, 1976). 600-1000µg of total protein was incubated with 10µL of α-Myc agarose beads or α-HA agarose beads in microcentrifuge tubes, gently rocking at 4°C overnight. Tubes were then centrifuged at 2,000 x g for 1min, and all protein extract removed. Beads were washed twice with HEPES wash buffer for 3min each, and finally resuspended in 15µL 2X LSB. Samples were boiled for 5min and spun-down before loading onto SDS-PAGE gels.

## **SDS-PAGE and western blot analyses**

Protein samples were brought to 1X LSB before loading onto 10% or 12.5% polyacrylamide gels for separation via SDS-PAGE (sodium dodecyl sulfate-polyacrylamide gel electrophoresis). Proteins were separated by running electrophoresis in SDS running buffer [25mM Tris-Cl, 192mM glycine, 0.1% SDS (w/v)] at 100V for 15min, then 150V for approximately 1hr. Proteins were then transferred to polyvinylidene fluoride (PVDF) membranes by running electrophoresis in ice cold transfer buffer [(pH 8.3) 25 mM Tris-Cl, 192 mM glycine, 20% methanol (v/v)] at 90V for 1¼hrs.

For western blotting, membranes were blocked in 5% non-fat milk in TBST [tris-buffered saline with Tween-20: 50mM Tris-Cl (pH 8.0), 150mM NaCl, 0.1% Tween-20 (v/v)] by medium rocking for 1hr, then washed with TBST three times for 5min. Membranes were incubated in primary antibody (1:5,000 in TBST for  $\alpha$ -ASK1 and  $\alpha$ -CUL1; 1:10,000 for  $\alpha$ -HA and  $\alpha$ -Myc) for 1-3hrs, or at 4°C for 12-16hrs by gently rocking, then washed with TBST three times for 5min. Membranes were then incubated in appropriate secondary antibody (1:10,000 in TBST) for 1hr, then washed with TBST 10min, then three times for 5min ( $\alpha$ -GFP used is a one-step antibody with horseradish peroxidase (HRP) conjugated, used at 1:10,000 in TBST, washed as above). Proteins of interest were detected by treating membranes with enhanced chemiluminescence (ECL) substrate, per manufacturer's instructions, and exposing membrane to X-ray film. Membranes were then stained with naphthol blue black (NBB), and Rubisco bands were used as a protein loading control.

### **Histochemical staining of GUS proteins**

The *HS:AXR3NT-GUS* transgene was previously described as inducible by a 37°C heat shock (Gray et al. 2001). Seedlings harboring *HS:AXR3NT-GUS* were grown on ATS media for 4 days before staining protocol. 10-20 seedlings of each line were placed in sterile DI water in 12-well plates and gently rocked at room temperature for 1hr to acclimate seedlings to liquid environment. Plates were then placed at 37°C and gently rocked for 2¼hrs to induce *AXR3NT-GUS* expression. Immediately after heat shock or at indicated timepoints, seedlings were placed in fixer solution [0.3% formaldehyde, 10mM 2-(N-morpholino)ethanesulfonic acid (MES), 0.3M mannitol] and vacuum infiltrated for 10min, followed by 30min gently rocking at room temperature. Seedlings were then washed by gently rocking in phosphate wash buffer [100mM Na<sub>2</sub>HPO<sub>4</sub>, pH 7.0] three times for 5min. Seedlings were stained by vacuum infiltrating for 15min with staining solution [100mM Na<sub>2</sub>HPO<sub>4</sub> (pH 7.0), 1 mM potassium ferrocyanide, 1 mM potassium ferricyanide, 10mM EDTA, 0.1M 5-Bromo-4-chloro-3-indoxyl-beta-D-glucuronide cyclohexylammonium salt, 0.1% Triton X-100 (v/v)] as described by Jefferson (1987), then kept at 37°C in darkness for 12-16hrs to develop blue color.

### **Root growth assay**

Sterilized seeds were germinated on ATS media for 4 days, then at least 8 seedlings from each line were transferred onto either ATS media plates supplemented with indicated concentrations of IAA, 2,4-D, Picloram, Methyl Jasmonate, or mock plates containing the respective chemical solvent. New root growth was measured after an additional 4 days.

Average percent root growth inhibition was calculated as follows:

$$\% \text{ Root Growth Inhibition} = \frac{\sum \left[ \frac{(\text{avg. control root length}) - (\text{treatment root length})}{(\text{avg. control root length})} * 100 \right]}{n}$$

Error bars in all graphs represent the standard error of the mean, which were calculated as follows:

$$\text{Standard Error} = \frac{SD}{\sqrt{n}}$$

Significant differences between means were determined using one-way analysis of variance (ANOVA). Assays were repeated at least three times with similar results.

### **Plant imaging**

Images of GUS-stained seedlings were acquired using the Nikon SMZ1500 stereo microscope (Nikon, Melville, NY). Images of soil-grown plants were acquired using Pentax K10D DSLR camera (Pentax, Tokyo, Japan). Confocal images of fluorescent *DII-Venus* protein were acquired using the Olympus FV1000 confocal microscope, and images were analyzed using Olympus Fluoview software (Olympus, Melville, NY) (Excitation 515nm, Emission 528nm; 20X W, NA 0.95) and ImageJ. Z-stacks are composite images of 10 successive slices of entire root tips. Image acquisition settings were kept constant within assays.

For hypocotyl elongation assays, images of hypocotyls were taken using the Nikon SMZ1500 stereo microscope, with millimeter scales in the frame. Hypocotyl lengths were measured using ImageJ software.

### III. RESULTS

#### **IBR5 interacts with ASK1 *in vitro***

To further test if IBR5 interacts with ASK1, *in vitro* pull-downs were performed using GST-ASK1 fusion protein expressed in *E. coli* and a MYC-tagged version of IBR5 (*35S:IBR5-Myc*) constitutively expressed in transgenic plants. GST-ASK1 was bound to glutathione agarose, and agarose was incubated in *35S:IBR5-Myc* protein extract. Bound proteins were analyzed by western blot using  $\alpha$ -ASK1 antibody, showing that IBR5 and ASK1 interact *in vitro* (Fig. 3a). To test the possibility that IBR5 is a substrate for SCF<sup>TIR1/AFBs</sup>, GST-ASK1 pulldowns were performed in the presence of auxin, showing that the interaction between IBR5 and ASK1 *in vitro* was unaffected by auxin. (Fig. 3b).

In order to confirm that IBR5 interacts with ASK1 *in vivo*, co-immunoprecipitation (Co-IP) assays were performed. *35S:IBR5-Myc* protein was immunoprecipitated from protein extracts using  $\alpha$ -Myc agarose, and western blots were probed with  $\alpha$ -ASK1 antibody. This Co-IP was unable to detect any interaction between IBR5 and ASK1 (Fig 4).

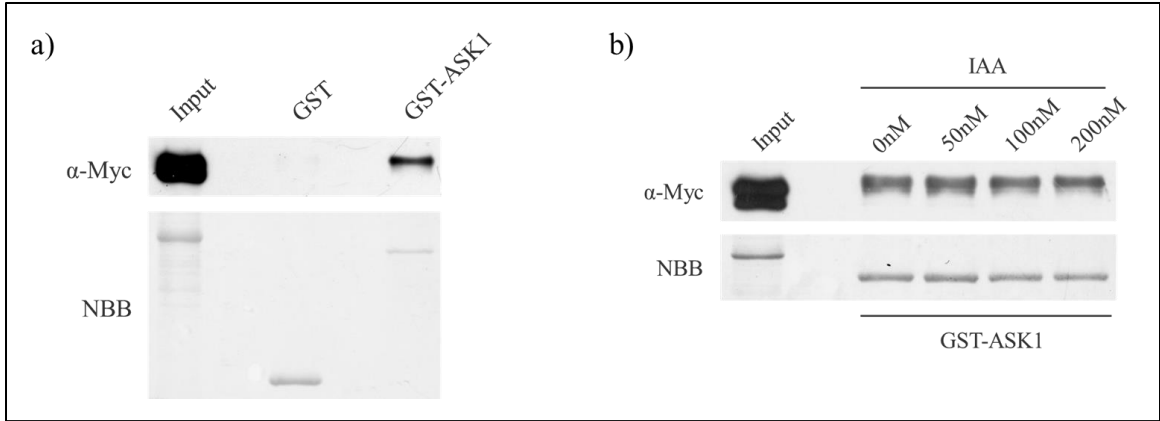


**Figure 3. IBR5 interacts with ASK1 *in vitro* independently of auxin.** a) Western blot analysis of GST Pull-down with recombinant GST-ASK1 expressed in *E. coli* bound to glutathione agarose and incubated with *35S*:IBR5-Myc protein. Proteins pulled down were detected with Myc antibody. b) GST Pull-down performed as in (a) in presence of mock or increasing concentrations of IAA in the incubation and wash steps. Membranes were visualized by staining blot with naphthol blue black (NBB).

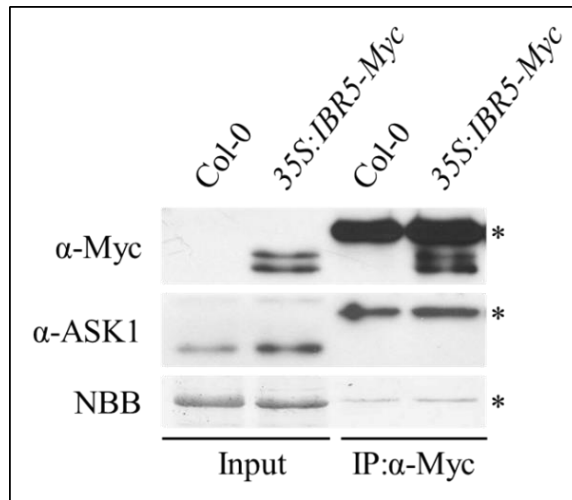


**Figure 4. IBR5-ASK1 interaction was not detected *in vivo* using Co-IP.**

Co-immunoprecipitation performed by incubating protein extracts from 10-day old Col-0 or *35S*:IBR5-Myc seedlings with  $\alpha$ -Myc agarose beads. Beads were washed, and immunoprecipitated proteins were detected with Myc and ASK1 antibodies. Experiment was performed three times with similar results. (\*) Asterisks indicate non-specific bands in IP lanes. NBB = naphthol blue black.

## IBR5 regulates steady state levels of SCF<sup>TIR1</sup> subunits

To determine the relevance of the interaction between IBR5 and ASK1, this study explored ways in which IBR5 may be involved in regulating SCF<sup>TIR1</sup>. The components of SCF<sup>TIR1</sup>, CUL1, ASK1 and TIR1, are shown to degraded through the 26S proteasomal pathway (Stuttman et al. 2009). To confirm this in an *in vitro* system, Col-0 proteins were incubated with or without MG132 at room temperature for 3hrs (Fig. 5a). MG132 treatment was effective at stabilizing ASK1, and to a lesser degree CUL1 (Fig. 5b).

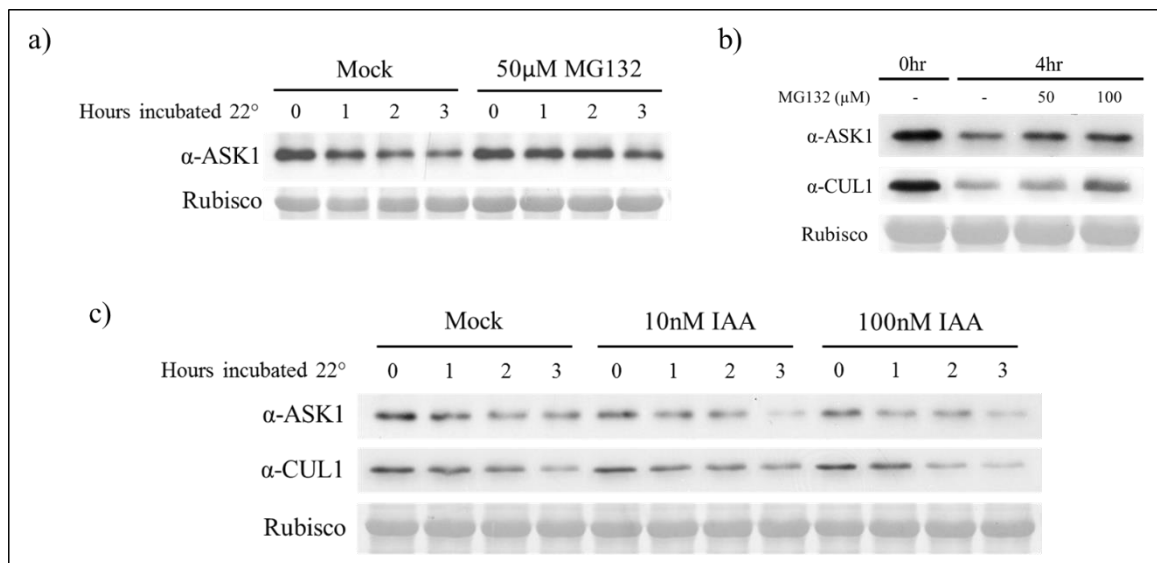


**Figure 5. ASK1 and CUL1 are degraded *in vitro* via the 26S proteasome.** a,b,c) Western blot analysis of 10-day old seedling protein extract with ASK1 and CUL1 antibodies. Col-0 total protein was extracted in native extraction buffer, aliquots were incubated at 22°C with indicated concentrations of MG132 or with an equivalent volume of DMSO (a,b), or with IAA or equivalent volume of ethanol (c). Rubisco is used as loading control.

Western blots of protein extracted from seedlings showed that the protein levels of ASK1, but not CUL1, are elevated in 3 different *ibr5* mutant alleles, and also in *35S:IBR5-Myc* (Fig. 6a,b). To test TIR1 protein levels, *ibr5* mutant lines were crossed into the transgenic line *TIR1:TIR1-HA* (in *tir1-1* background). Homozygous lines were

generated, and proteins were extracted from seedling roots and shoots and analyzed by western blot. As expected, *sgt1b-4*, a splice site mutant of SGT1b that is resistant to natural and synthetic auxins (Walsh et al. 2006), had a decreased level of TIR1 protein, but only in root tissue (Fig. 6c,d). In both root and shoot tissues, *ibr5* mutants have significantly increased levels of TIR1 protein compared to Col-0 (Fig. 6c,d). Interestingly, *35S:IBR5-Myc* also has elevated levels of TIR1 in shoot tissue, but wild-type levels of TIR1 in root tissue (Fig. 6c,d).

*CORONATINE-INSENSITIVE1 (COI1)* is an F-box protein required for jasmonic acid (JA) signaling that is similar to TIR1 in nucleotide sequence (Ruegger et al. 1998). It is possible that COI1 and TIR1 are subjected to similar regulation by IBR5. Whether IBR5 is involved in JA signaling has remained an open question, however. Thus, a root growth assay was performed using inhibitory concentrations of methyl jasmonic acid (MeJA) on ATS media to test the role of IBR5 in the JA pathway. Root growth of *ibr5* mutants, as well as *35S:IBR5-Myc*, showed little to no altered response to MeJA compared to Col-0 (Fig. 7a,b).

In order to test whether ASK1 or TIR1 protein levels were increased due to gene expression, qPCR was performed using cDNA from 7-day old Col-0 and *ibr5* mutant seedlings. For the transgene *TIR1-HA*, with which TIR1 protein levels were observed, expression was marginally decreased in *ibr5-1* and *35S:IBR5-Myc* backgrounds compared to Col-0 (Fig. 8a,b). With the native *ASK1* gene, qPCR showed that expression is unchanged in *35S:IBR5-Myc* and *ibr5* mutants, except for *ibr5-4*, which shows a significant decrease in ASK1 expression compared to Col-0 (Fig. 9).

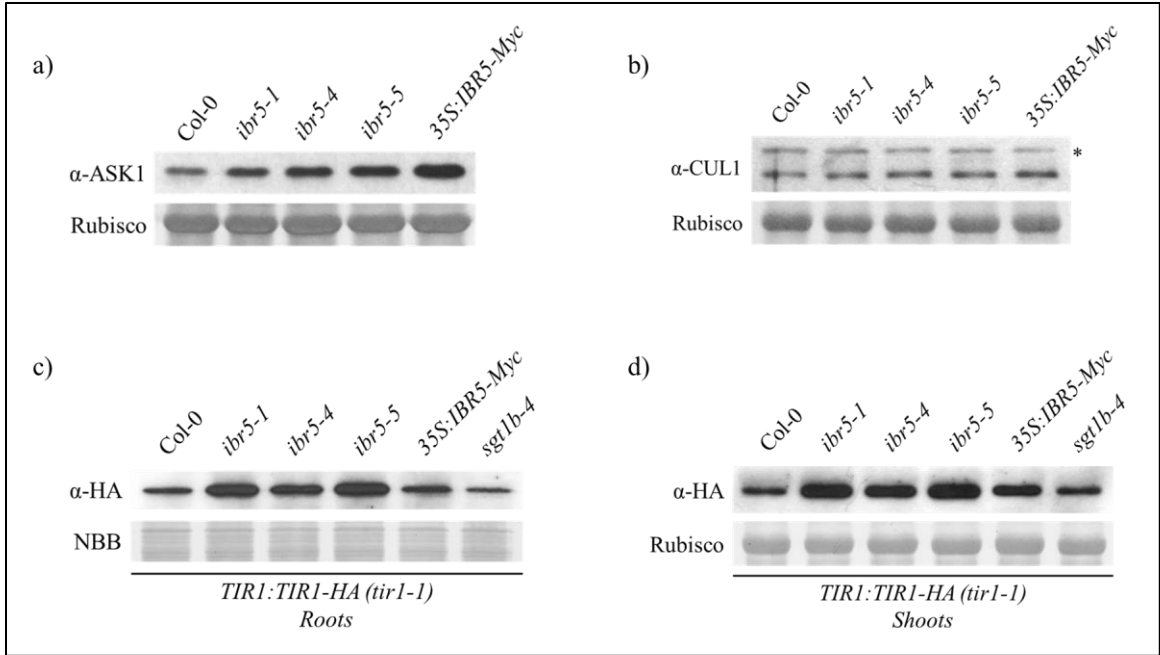


**Figure 6. IBR5 regulates steady state levels of ASK1 and TIR1.** a,b) Western blot analysis of 4-day old seedling protein extract with ASK1 (a) and CUL1 (b) antibodies. c,d) Western blot analysis of 6-day old root (c) and shoot (d) protein extract with HA antibody. Rubisco is used as loading control in (a,b,d), and membrane stained with NBB was used as loading control in (c). (\*) Asterisk indicates rubylated form of CUL1.

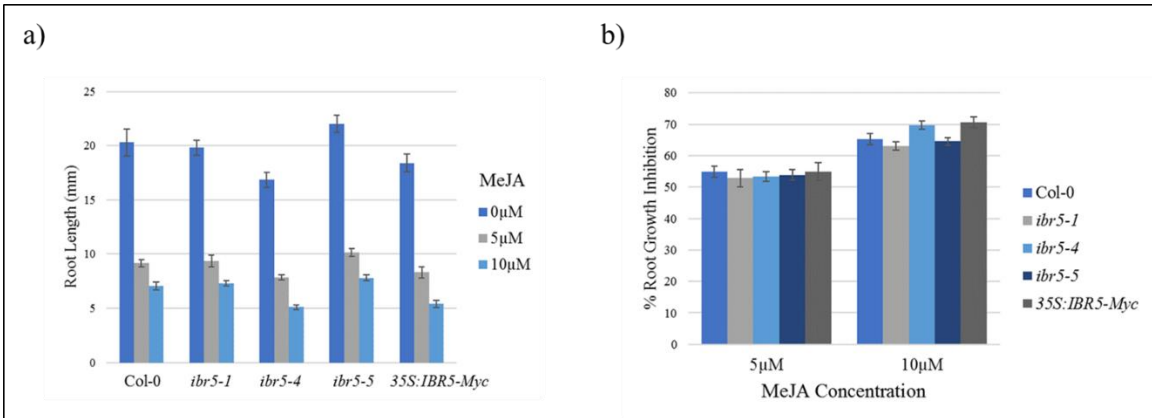


**Figure 7. *ibr5* mutants show no altered response to methyl jasmonic acid.** a) 4-day old seedlings were transferred to ATS media containing mock (EtOH) or MeJA, and new growth was measured after 4 more days. b) Percent root growth inhibition was calculated relative to mock treatment. Error bars indicate standard error of the mean.

Considering TIR1 is necessary for reception of auxin, albeit partially redundantly with AFBs, the abundance of TIR1 should correlate with a plant's ability to respond to the cellular signal of auxin. Thus, the regulation of TIR1 protein levels by IBR5 was explored. Despite having elevated TIR1 protein levels, *ibr5* mutants are resistant to auxin, and *35S:IBR5-Myc* has no significant effect on auxin sensitivity compared to Col-0, nor normal root growth (Fig. 10a,b).

### **26S proteasomal degradation and HSP90-mediated stabilization of TIR1 protein levels are unaffected by IBR5**

TIR1 is regulated by the 26S proteasome (Stuttman et al. 2009). Thus, it is possible that IBR5 is involved in the proteasomal degradation of TIR1. When seedlings were treated with MG132, an inhibitor of the 26S proteasome, each background exhibited a significant increase in TIR1 protein level, relatively similar to the increase seen in the wild type background (Fig. 11a). *In vitro* degradation of TIR1 was tested in *ibr5-1* and *35S:IBR5-Myc* with an equalized beginning amount of TIR1-HA protein, and no difference was observed relative to Col-0 (Fig. 11b). Heat stress, or an increase from 22°C to 30°C, stabilizes TIR1 in an HSP90-dependent manner (Wang et al. 2016). To determine if IBR5 is involved in heat-stress induced stabilization of TIR1 protein, *TIR1:TIR1-HA (tir1-1)* seedlings were exposed to heat stress for 2hrs, and TIR1 levels in *ibr5-1* and *35S:IBR5-Myc* backgrounds increased proportionately to Col-0 (Fig. 12a). The same concomitant increase was observed when seedlings were heat-shocked at 37°C for 2hrs (Fig. 12b).

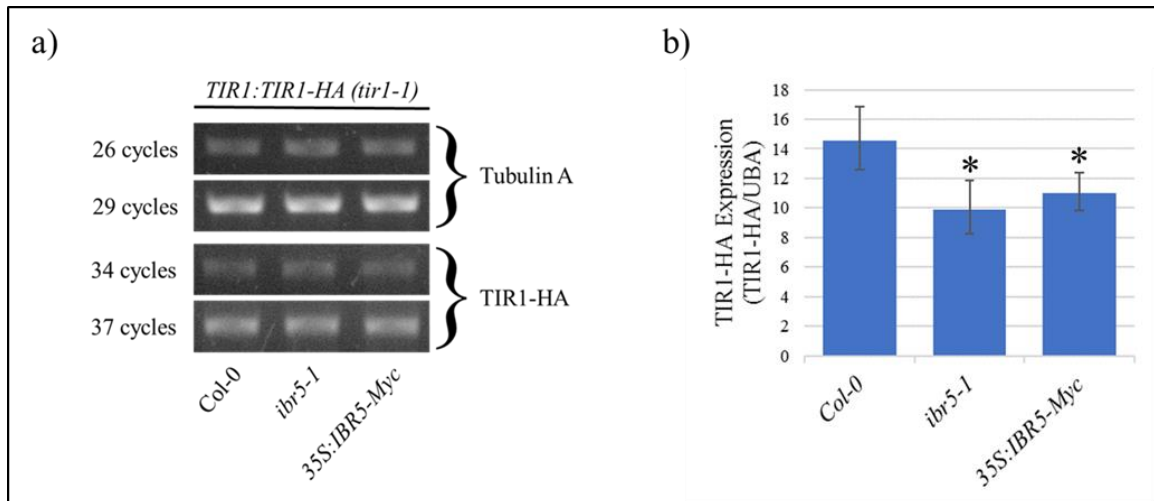


**Figure 8. Analysis of *TIR1* gene expression in *ibr5-1* mutant and overexpression lines.** a) Reverse-transcriptase PCR (RT-PCR) performed using cDNA prepared from RNA extracted from 7-day old seedlings expressing *TIR1;TIR1-HA (tir1-1)*. Cycle numbers indicate PCR program used  $\alpha$ -Tubulin (*TUA*) was used as a reference gene. Assay was performed three times with similar results b) qPCR analysis of cDNA samples as in (a) using SYBR Green reagent mixture. Ubiquitin-associated protein (*UBA*) was used as a reference gene. Gene expression was analyzed using the Livak method and is presented relative to *UBA* expression. Assay was performed in three biological replicates with similar results. Error bars indicate standard error of the mean. (\*) Asterisks indicate significant differences from Col-0 (T-test, p < 0.01).

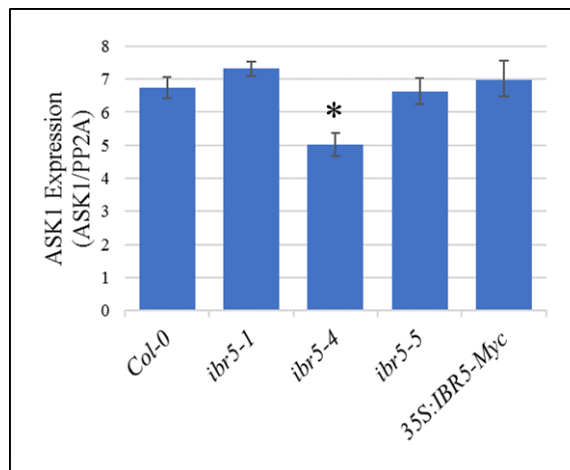


**Figure 9. qPCR analysis of *ASK1* gene expression in *ibr5* mutant and overexpression lines.** qPCR performed using cDNA prepared from RNA extracted from 7-day old seedlings, using SYBR Green reagent mixture. *PP2A* was used as a reference gene. Gene expression was analyzed using the Livak method and is presented relative to *PP2A* expression. Assay was performed in three biological replicates with similar results. Error bars indicate standard error of the mean. (\*) Asterisk indicates significant difference from Col-0 (T-test, p < 0.01).

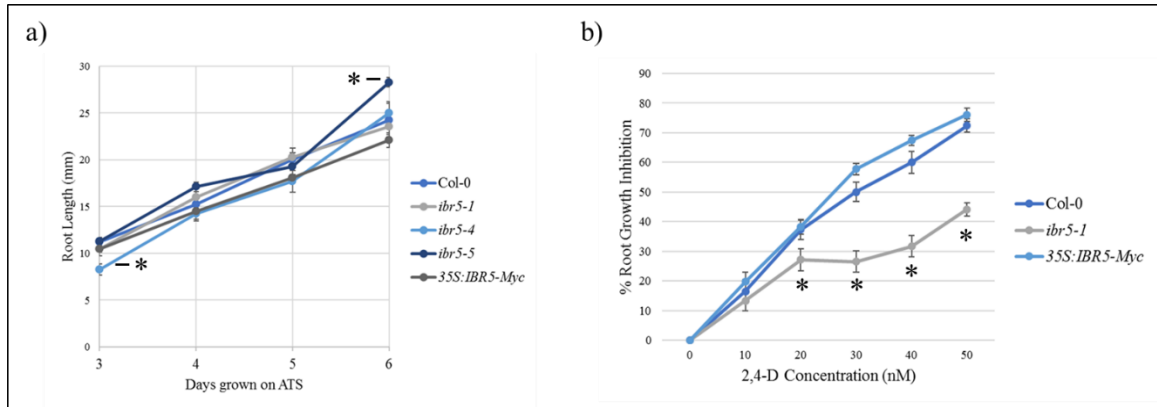


**Figure 10. *35S:IBR5-Myc* is not hypersensitive to auxin.** a) Sterilized seeds were vernalized and grown on ATS media for indicated number of days, and root length was measured. b) 4-day old seedlings were transferred to ATS media containing mock (EtOH) or indicated concentrations of 2,4-D, and new growth was measured after 4 more days. Percent root growth inhibition was calculated relative to mock treatment. (\*) Asterisks indicate significant differences from Col-0 calculated using one-way ANOVA ( $p < 0.01$ ). Assays were performed three times with similar results.

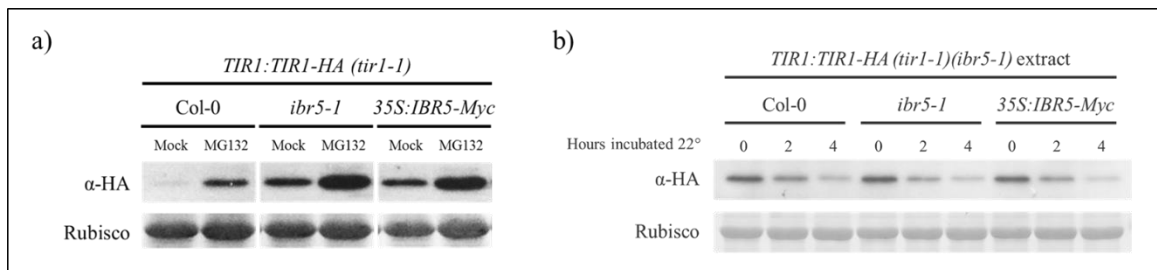


**Figure 11. Degradation of TIR1 in *ibr5-1* and *35S:IBR5-Myc*.** a) 26S proteasomal degradation was assessed by treating 6-day old seedlings with 50 $\mu$ M MG132 for 4 hours. Protein was extracted and analyzed via western blotting using HA antibody. b) Protein extract from *TIR1:TIR1-HA (tir1-1)* in *ibr5-1* background was co-incubated at 22°C in 10-day old Col-0, *ibr5-1*, or *35S:IBR5-Myc* protein extracts. Samples were taken at indicated timepoints and analyzed as in (a). Rubisco is used as loading control.

To further test if IBR5 affects HSP90-mediated stabilization of TIR1, the chemical geldanamycin (GDA), a highly specific inhibitor of HSP90, was used (Saibil 2013; Wang et al. 2016). *TIR1:TIR1-HA (tir1-1)* seedlings treated with 10 $\mu$ M GDA for 24hrs experienced a significant reduction in TIR1 levels in *ibr5-1* and *35S:IBR5-Myc* backgrounds, similarly to Col-0 (Fig. 12c). To test if HSP90 is involved with IBR5 in regulating Aux/IAA degradation, a degradation assay was performed in the presence of GDA. The heat-shock inducible reporter construct *HS:AXR3NT-GUS* consists of the N-terminal domains I and II of IAA17 fused with  $\beta$ -glucuronidase (GUS), driven by the soybean heat-shock promoter (HS) (Gray et al. 2001). *HS:AXR3NT-GUS* was crossed into *ibr5-1* and *35S:IBR5-Myc* backgrounds. After inducing expression with 2hrs of heat-shock, the presence of GDA stabilized the Aux/IAA protein fragment AXR3NT in both backgrounds proportionately to Col-0 (Fig. 13).

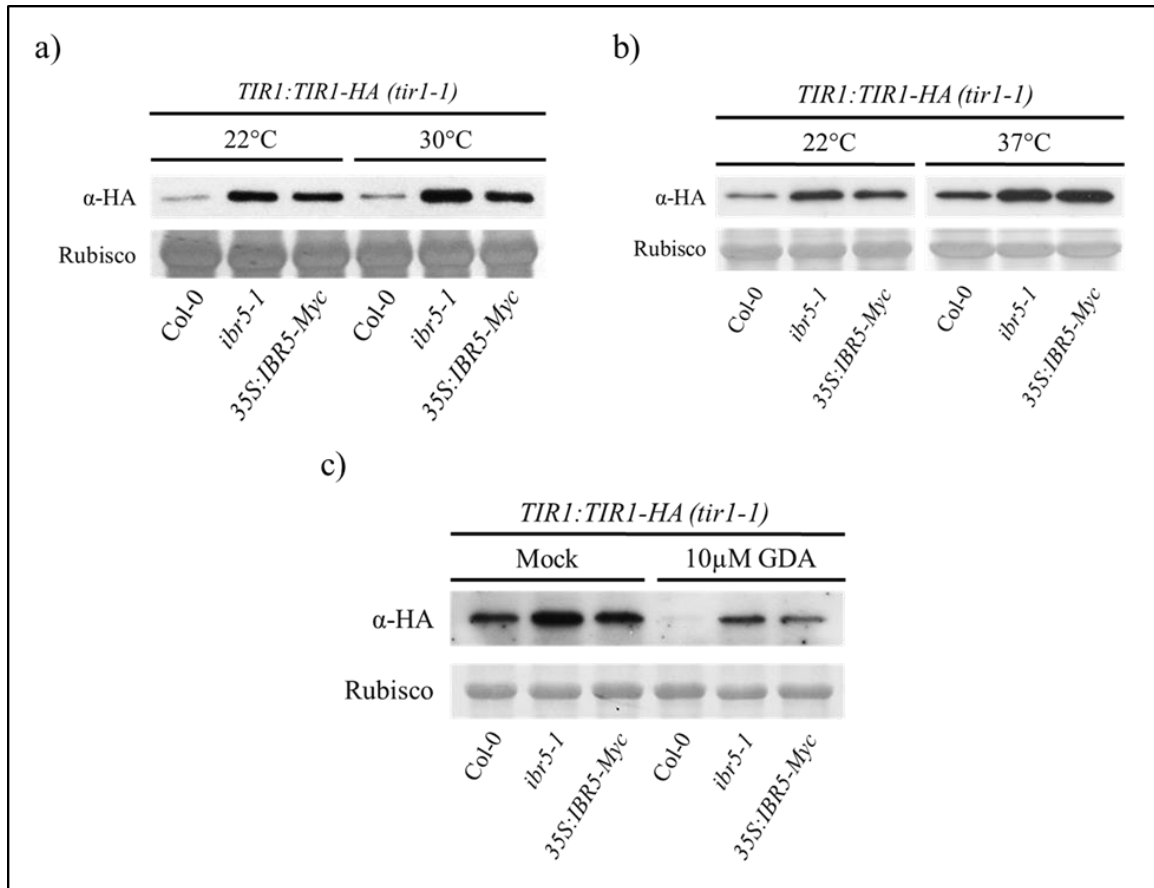


**Figure 12. Effects of heat stress on TIR1 protein.** a,b) 6-day old seedlings expressing *TIR1: TIR1-HA (tir1-1)* were incubated at room temperature (22°C), and 30 °C or 37 °C for 2 hours. Protein was extracted and analyzed via western blotting using HA antibody. c) *TIR1: TIR1-HA (tir1-1)* seedlings were incubated with 10µM geldanamycin (GDA; specific inhibitor of HSP90) or mock (DMSO) for 24hrs, and protein sample analyzed as in (a,b). Rubisco is used as loading control.

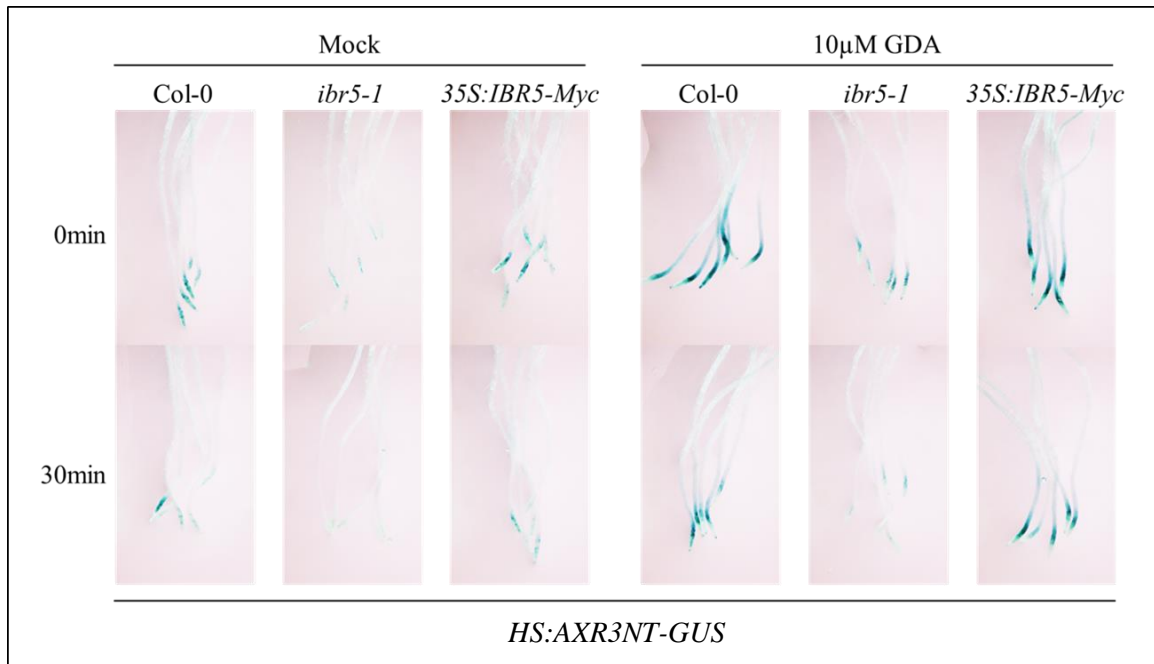


**Figure 13. GDA stabilizes Aux/IAA proteins irrespective of IBR5 activity.** 4-day old *HS:AXR3NT-GUS* seedlings were heat-shocked at 37°C for 2hrs in the presence of mock (DMSO) or 10µM GDA in sterile water, then fixed and stained with X-gluc at indicated timepoints.

Heat stress in plants triggers hypocotyl elongation, and this response is dependent upon auxin signaling (Gray et al. 1998). A more recent study shows that this process is mediated by HSP90 (Wang et al. 2016). To test the role of IBR5 in this process, a hypocotyl elongation assay was performed. *ibr5* mutants that were grown for 6 days at 30°C had significantly shorter hypocotyls than Col-0 (Fig. 14a). Interestingly, *ibr5-4* seedlings had significant root inhibition at 30°C (Fig. 14b).

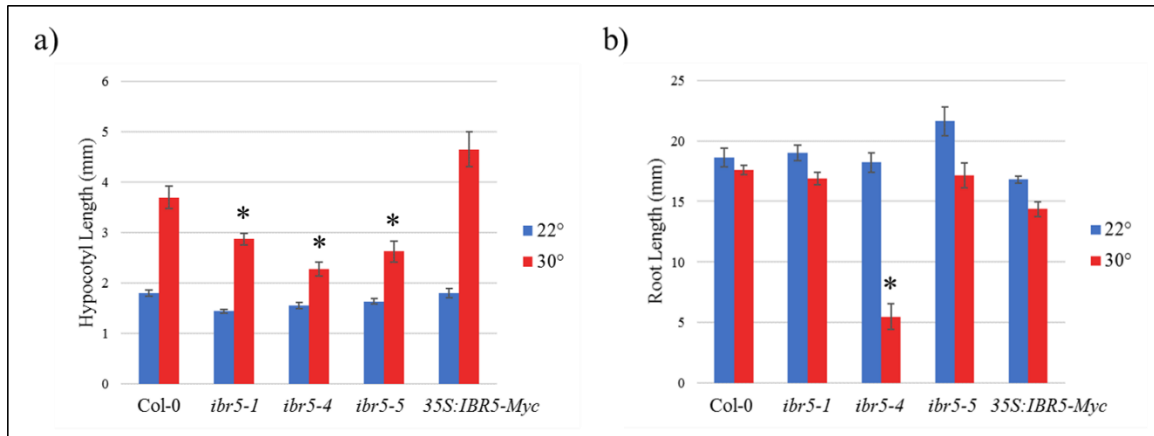


**Figure 14. IBR5 is involved in plant response to heat stress.** a,b) Sterilized seeds were vernalized and grown on ATS media for 6 days at 22°C or 30°C, after which hypocotyls (a) and roots (b) were measured. Error bars indicate standard error of the mean. (\*) Asterisks indicate significant differences from Col-0 calculated using one-way ANOVA ( $p < 0.01$ ). Assays were performed three times with similar results.

### IBR5 regulates degradation of Aux/IAs in distinct ways

IBR5 has been shown to be involved in Aux/IAA degradation using *HS:AXR3NT-GUS*, and *IAA28:IAA28-Myc*, both of which are destabilized in *ibr5-1* background (Strader, Monroe-Augustus, Bartel 2008). This was also observed with *HS:AXR3NT-GUS* in *ibr5-4* (Jayaweera et al. 2014), and in this study in *ibr5-5* (Fig. 15). *ibr5-5* is a splice-site mutant that is resistant to auxin similar to *ibr5-1* (Jayaweera et al. 2014). Since the initial amount of GUS present in the *ibr5* mutants is decreased, it is possible that *AXR3NT-GUS* is not being expressed to the same level as in Col-0. However, qPCR analysis showed that *AXR3NT-GUS* expression in seedling roots is induced as expected by heat shock (Fig. 16a) and is similar across all lines immediately following heat shock (Fig. 16b).

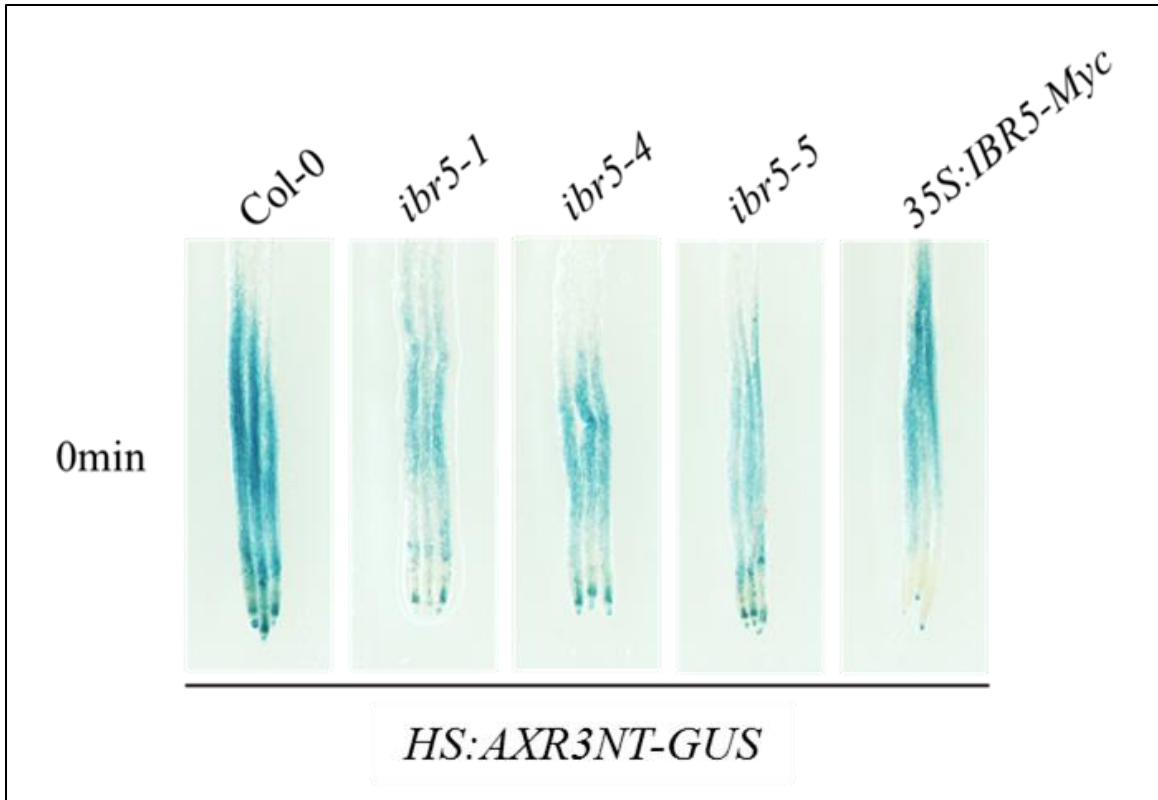


**Figure 15. *ibr5* mutants exhibit increased Aux/IAA degradation using *HS:AXR3NT-GUS* reporter line.** 4-day old *HS:AXR3NT-GUS* seedlings were heat-shocked at 37°C for 2hrs in sterile water. Seedlings were then fixed and stained with X-gluc.

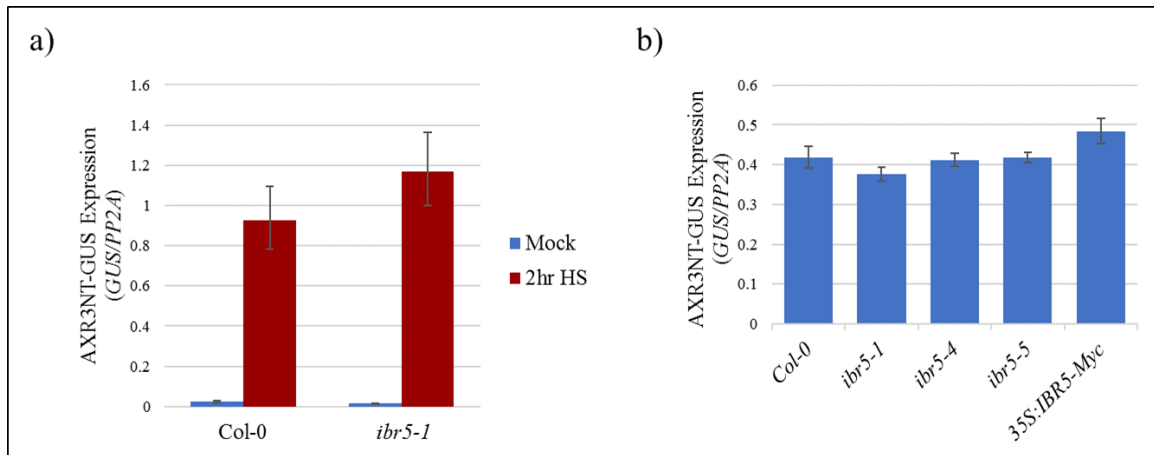


**Figure 16. qPCR analysis of heat shock-inducible *HS:AXR3NT-GUS* in *ibr5* mutants.** a,b) Roots from 4-day old *HS:AXR3NT-GUS* seedlings were heat-shocked at 37°C for 2hrs in sterile water. a) Tissue was flash frozen immediately following heat shock, or 22°C mock treatment, and RNA was extracted for cDNA synthesis, followed by qPCR. b) Tissue was flash frozen immediately following heat shock, and RNA was extracted for cDNA synthesis, followed by qPCR. *PP2A* was used as a reference gene. Assays were performed in three biological replicates with similar results. Error bars indicate standard error of the mean. No significant difference in expression was observed compared to Col-0 in (a) or (b) (T-test,  $p < 0.01$ ).

A recently developed reporter gene, *35S:DII-Venus*, has been used to sense auxin responses *in vivo* (Brunoud et al. 2012). This reporter gene was constructed by fusing the fluorescent protein “Venus” with a nuclear localization signal (NLS) to the conserved domain II (DII) of Aux/IAA proteins, which functions as the degron motif required for binding to TIR1 in the presence of auxin, and subsequent degradation. The *35S:DII-Venus* line was crossed with *ibr5* mutants and *35S:IBR5-Myc* to further assess the stability of Aux/IAA proteins in these backgrounds. Epifluorescent microscopy (Fig. 17a), as well as western blotting of seedling protein extract (Fig. 17b), showed that *DII-Venus* was relatively stabilized in *ibr5* mutant backgrounds compared to Col-0, while *35S:IBR5-Myc* showed a dramatic stabilization of *DII-Venus*. Z-stacks acquired using

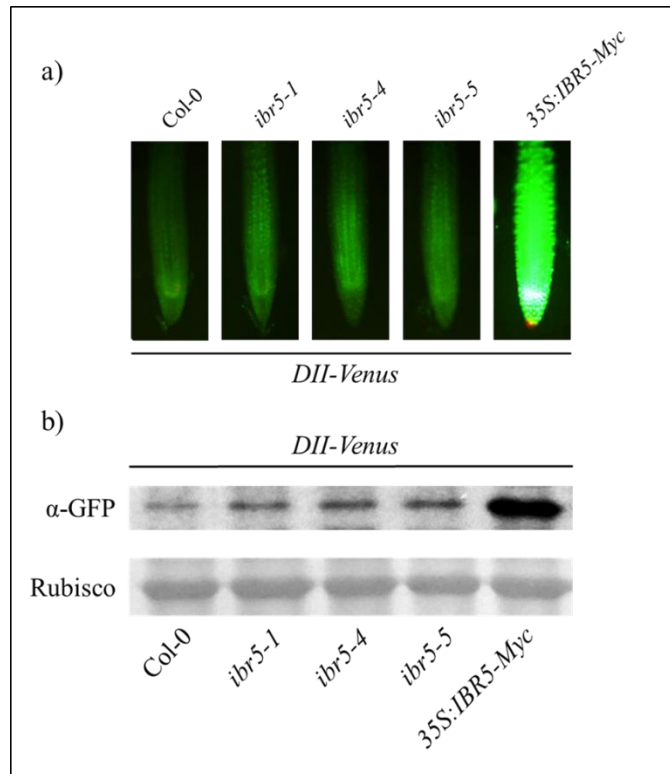


**Figure 17. 35S:*DII-Venus* is stabilized in *ibr5* mutant and 35S:*IBR5-Myc* backgrounds.** a) 6-day old *DII-Venus* seedling roots were imaged using epifluorescent microscopy. b) Protein was extracted from 6-day old *DII-Venus* seedlings and analyzed with western blotting using GFP antibody. Rubisco protein is used as loading control. Experiment was repeated three times with similar results.

confocal microscopy showed the difference between Col-0 and *ibr5* mutants clearly (Fig. 18).

Since two different Aux/IAA reporter gene constructs show conflicting results regarding Aux/IAA stability in *ibr5* mutant backgrounds, the question was raised whether IBR5 directly interacts with Aux/IAA proteins to regulate their stability. GST pull-downs were performed *in vitro* to test this hypothesis with several GST-fused Aux/IAA proteins. IBR5-Myc appeared to interact very weakly with only GST-IAA12, and not at all with GST-IAA7 or GST-IAA14 (Fig. 19a,b).

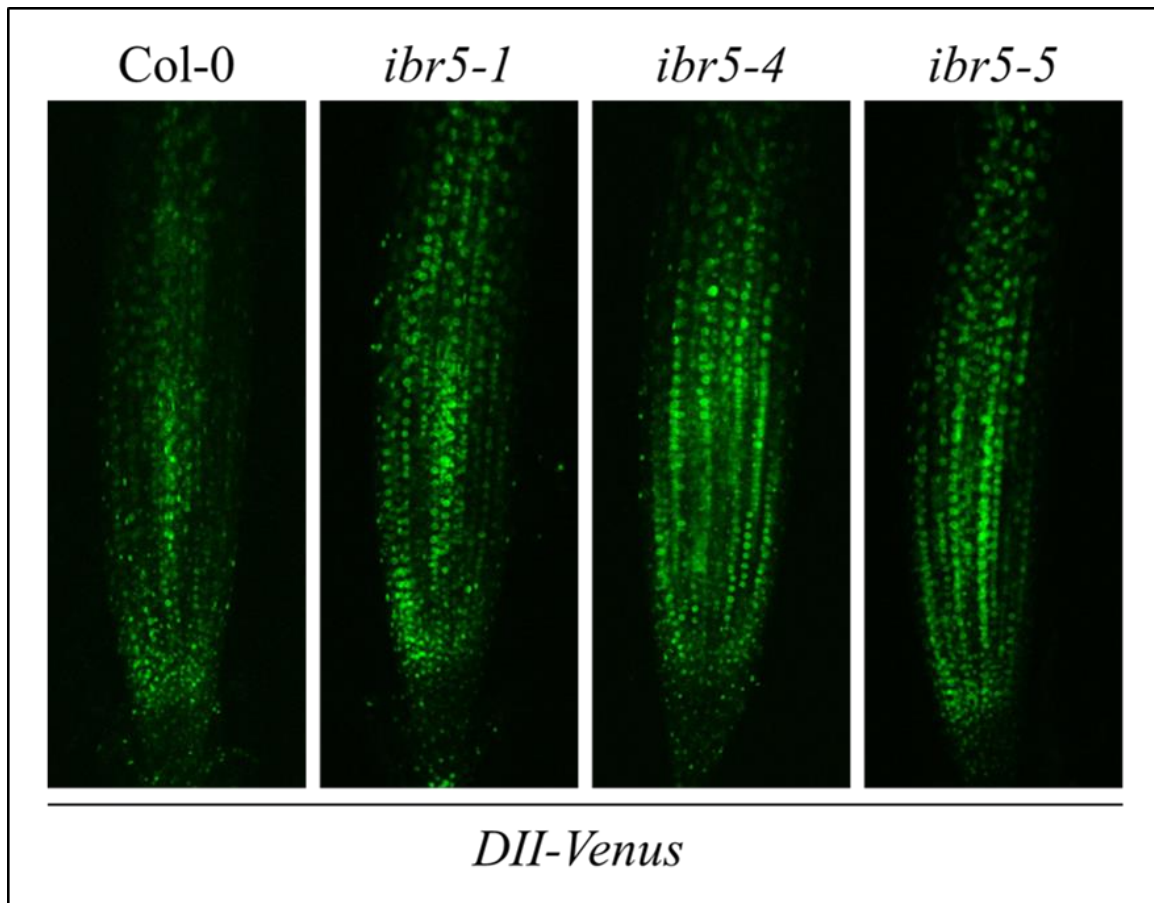


**Figure 18. Confocal Z-stack images show 35S:DII-Venus stabilization in *ibr5* mutants.** Z-stack images of *DII-Venus* in root tips of Col-0 and *ibr5* mutant backgrounds. Z-stacks are composite images of 10 successive slices through entire root tips of 6-day old seedlings. Images were acquired three times with similar results.

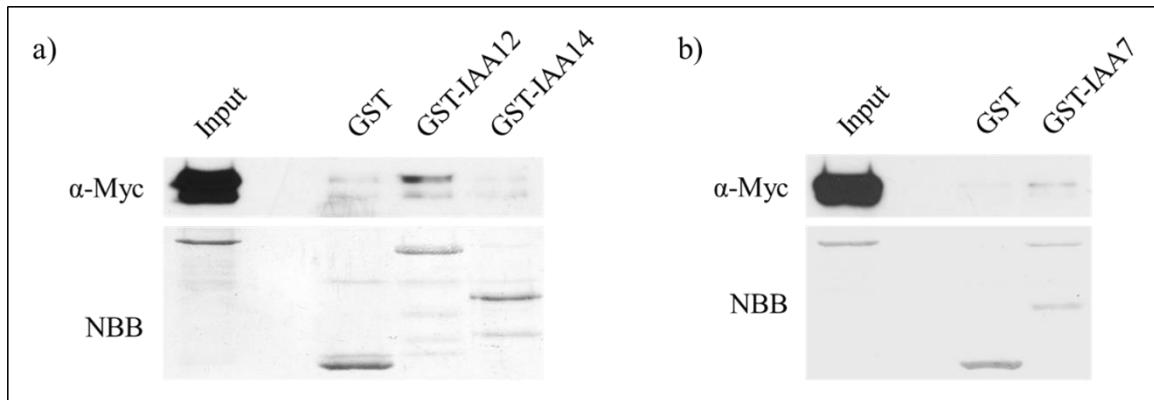


**Figure 19. IBR5 does not interact significantly with Aux/IAA proteins *in vitro*.** a,b) Western blot analysis of GST Pull-down with recombinant GST-IAA7/-IAA12/-IAA14 expressed in *E. coli* bound to glutathione agarose and incubated with *35S:IBR5-Myc* protein. Proteins pulled down were detected with Myc antibody. Multiple bands are present in GST-IAA lanes due to fracturing of protein that occurs during sonification, however these fragments retain GST tag and are still pulled down. NBB = Naphthol blue black.

### Genetic interaction between SGT1b and IBR5

Both IBR5 and SGT1b mutants have auxin resistance and were shown to interact in regulating disease resistance (Liu et al. 2015). Since both these proteins regulate TIR1 protein stability (Fig. 6c,d), it is possible they work together to regulate auxin signaling through TIR1. In order to assess the genetic interaction between IBR5 and SGT1b, double mutants were generated between *sgt1b-4*, and alleles *ibr5-1*, *ibr5-4*, and *ibr5-5*, as well as *35S:IBR5-Myc*. *sgt1b-4* is a splice site mutant of SGT1b that is resistant to natural and synthetic auxins (Walsh et al. 2006). Overall, the double mutants exhibited phenotypes intermediate between phenotypes from either single mutant. With 3-week old plants, *ibr5-1* and *ibr5-5* both contributed serrated leaf margins to double mutants, while *ibr5-4* and *35S:IBR5-Myc* double mutants appear to change little compared to single mutants (Fig. 20). *ibr5-5* plants have relatively long serrated leaves, but *ibr5-5, sgt1b-4* plants have a reduced stature compared to Col-0 (Fig. 20).

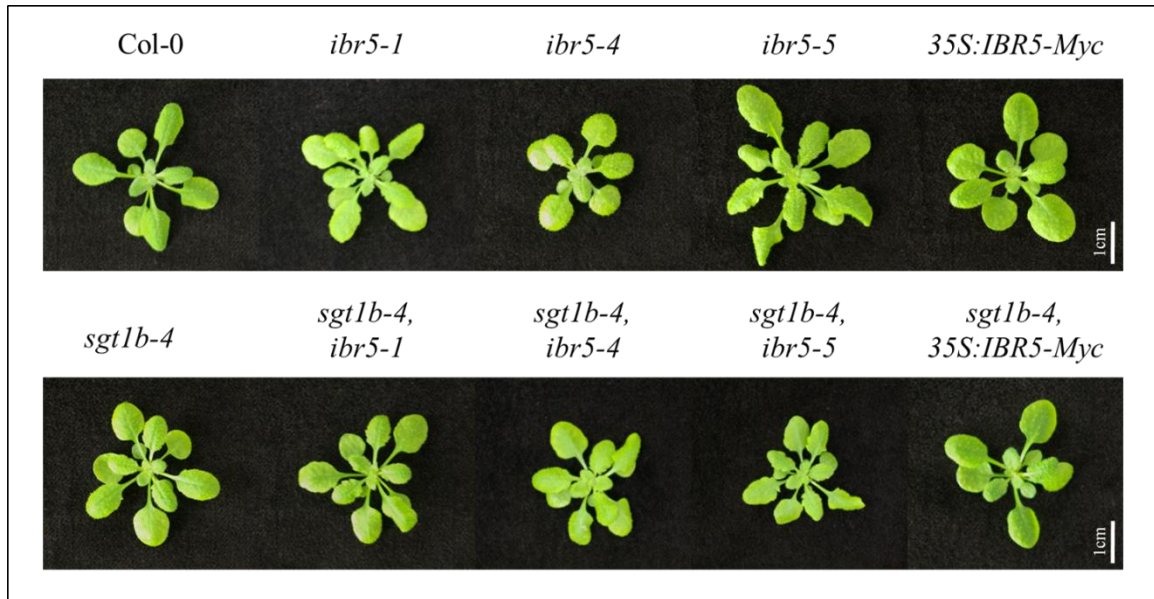


**Figure 20. 3-week old phenotypes of *ibr5*, *sgt1b-4* double mutant lines.** Double mutant lines were generated by crossing and genotyping to find homozygous lines. Seeds were sown on moist soil, vernalized for 2 days, then grown for 3 weeks at 22°C in long-day conditions (16hr day/8hr night). Scale bar = 1cm.

When seedlings were transferred onto media containing 70nM 2,4-D, Col-0 exhibited strongly inhibited root growth, while *ibr5* mutants and *sgt1b-4* were significantly more resistant, with *sgt1b-4* being the most resistant (Fig. 21a,b). In the case of the double mutants, all three crosses with *ibr5* alleles resulted in moderate increases in resistance to 2,4-D. While it has been shown that the synthetic auxin 2,4-D is a reliable surrogate for the action of IAA (Dharmasiri et al. 2005), there is plenty of evidence that synthetic auxins produce unique responses in the plant (Pufky et al. 2003; Walsh et al. 2006). Thus, this genetic interaction was also tested with IAA and the synthetic auxin, picloram.

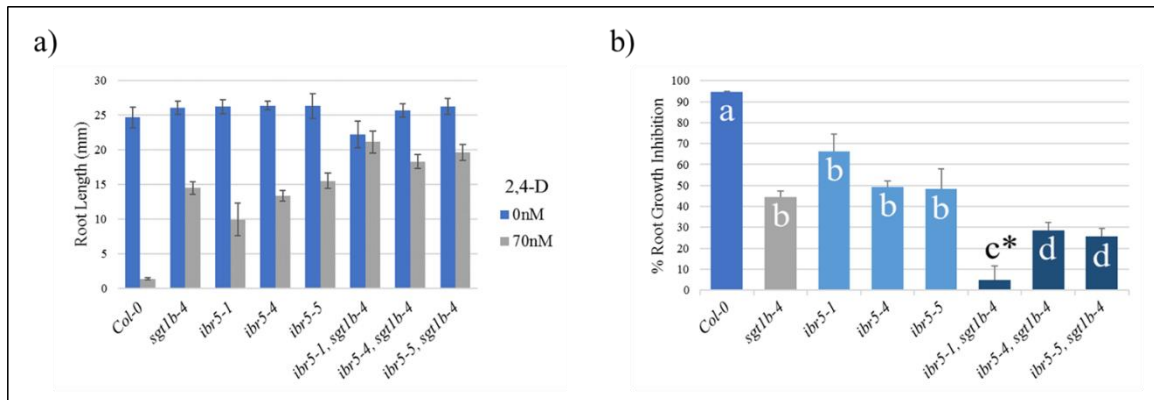


**Figure 21. *ibr5*, *sgt1b-4* double mutant lines have increased resistance to 2,4-D compared to single mutants.** a) 4-day old seedlings were transferred to ATS media containing mock (EtOH) or 70nM 2,4-D, and new growth was measured after 4 more days. b) Percent root growth inhibition was calculated relative to mock treatment. Colors are to segregate single and double mutants. Error bars indicate standard error of the mean. Letters indicate significant differences in percent inhibition using one-way ANOVA ( $p < 0.05$ ). \*Letter “c” is significantly different from “a” and “b” at  $p < 0.01$ . The assay was performed three times with similar results.

When *ibr5*, *sgt1b-4* double mutant lines were transferred to media containing IAA, both *ibr5-1*, and *ibr5-5* alleles resulted in a moderate increase in resistance to root growth inhibition compared to single mutants (Fig. 22a,c), while *ibr5-4* contributed only a slight increase in resistance (Fig. 22b). *35S:IBR5-Myc*, which has wild-type resistance to IAA, had no effect on *sgt1b-4* resistance (Fig. 22d). These results are similar, but not exactly the same as those seen with 2,4-D resistance.

When grown on media containing picloram, *sgt1b-4* is highly resistance to root growth inhibition, while *ibr5* mutants are only slightly resistant, and *35S:IBR5-Myc* has wild-type sensitivity. *ibr5*, *sgt1b-4* double mutant lines appear to each have different effects on picloram resistance compared to single mutants. Crosses with *ibr5-1* or *ibr5-5* alleles resulted in virtually no change to *sgt1b-4* picloram resistance (Fig. 23a,c). On the other hand, crosses with *ibr5-4* and *35S:IBR5-Myc* resulted in a slight increase in

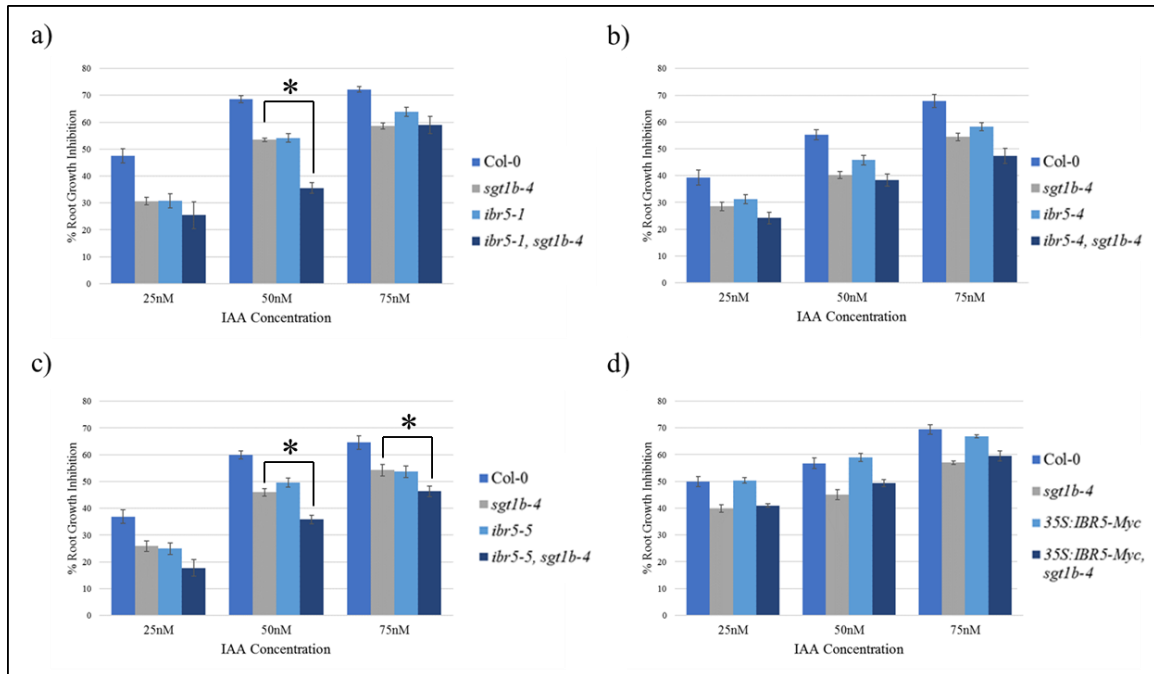


**Figure 22. *ibr5*, *sgt1b-4* double mutant lines have increased resistance to IAA compared to single mutants.** 4-day old seedlings were transferred to ATS media containing mock (EtOH) or indicated concentrations of IAA, and new growth was measured after 4 more days. Lines tested were Col-0, *sgt1b-4*, and single and double mutants of *ibr5-1* (a), *ibr5-4* (b), *ibr5-5* (c), or *35S:IBR5-Myc* (d). Percent root growth inhibition was calculated relative to mock treatment. Error bars indicate standard error of the mean. (\*) Asterisks indicate significant differences in percent inhibition using one-way ANOVA ( $p < 0.01$ ). The assay was performed three times with similar results.

picloram resistance compared to *sgt1b-4* single mutant (Fig. 23b,d). Interestingly, although *ibr5-1*, *sgt1b-4* double mutants have the same root growth resistance to picloram as *sgt1b-4*, their shoots are more resistant to the hypocotyl extension and cotyledon curling effects of picloram (Fig. 23e).

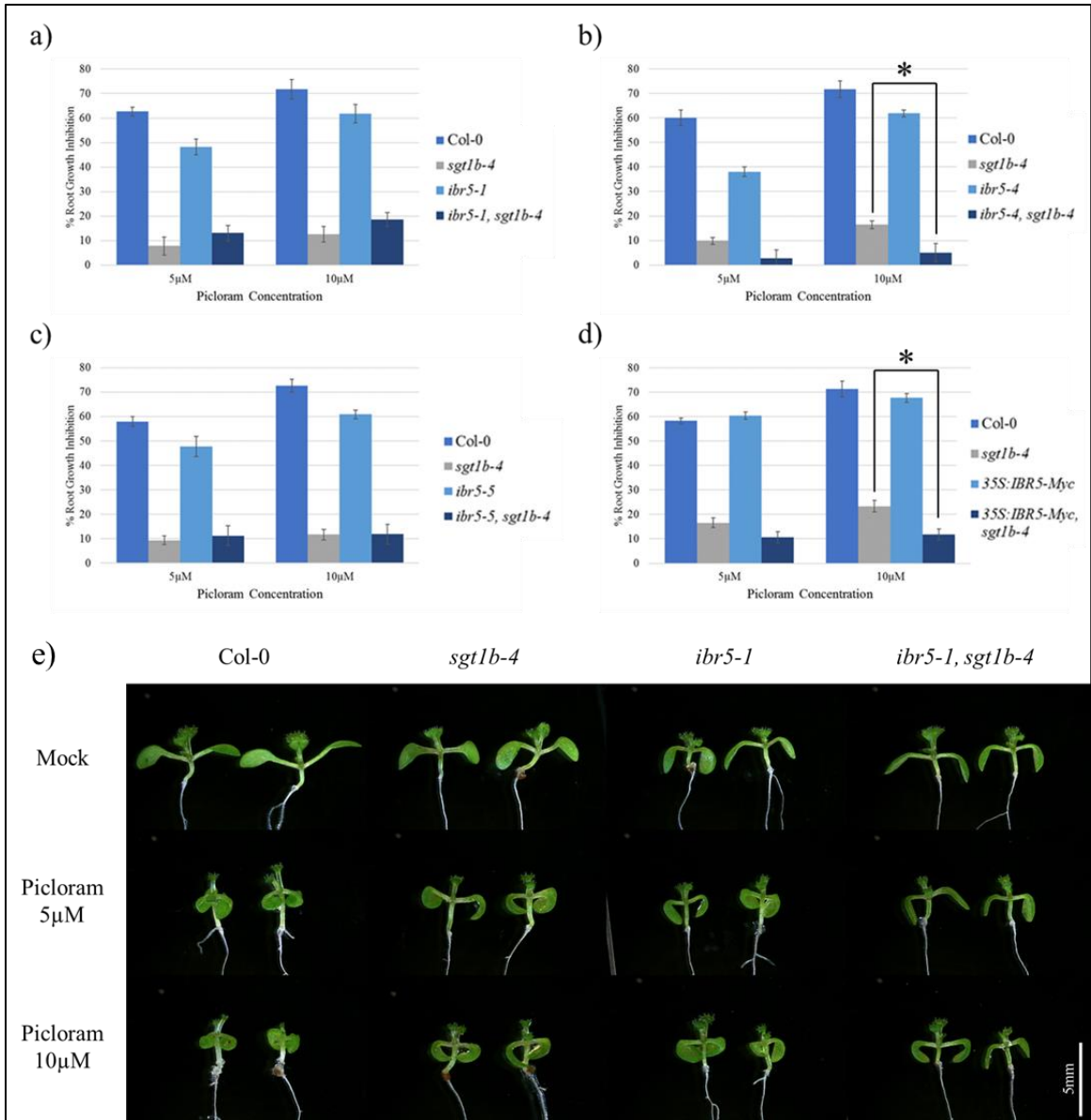


**Figure 23. *ibr5, sgt1b-4* double mutant lines have different effects on picloram resistance compared to single mutants.** a-d) 4-day old seedlings were transferred to ATS media containing mock (DMSO) or indicated concentrations of picloram, and new growth was measured after 4 more days. Lines tested were Col-0, *sgt1b-4*, and single and double mutants of *ibr5-1* (a,e), *ibr5-4* (b), *ibr5-5* (c), or *35S:IBR5-Myc* (d). Percent root growth inhibition was calculated relative to mock treatment. Error bars indicate standard error of the mean. (\*) Asterisks indicate significant differences in percent inhibition using one-way ANOVA ( $p < 0.01$ ). e) Shoot phenotypes of *ibr5-1, sgt1b-4* double mutants when grown as in (a). Assays were performed three times with similar results.

Since *ibr5* mutants and *35S:IBR5-Myc* lines have increased TIR1 protein levels, and *sgt1b-4* has decreased TIR1 protein levels, it is possible that these lines crossed could recover auxin response, conceivably by returning TIR1 levels close to those in wild-type. The effects of relative TIR1 protein levels on auxin resistance in the *sgt1b-4* background were tested. The transgenic line *TIR1:TIR1-HA* in Col-0 background was crossed into *sgt1b-4* and homozygous lines generated were subjected to a root growth assay on 2,4-D, alongside other *sgt1b-4* lines. The transgenic increase of TIR1 in *sgt1b-4* background recovered auxin sensitivity to wild-type levels (Fig. 24a,b). In contrast, double mutants of *sgt1b-4* with either *ibr5-1* or *35S:IBR5-Myc* do not recover auxin sensitivity to the *sgt1b-4* mutant (Fig. 22a,d; Fig. 23a,d,e; Fig. 24a,b).

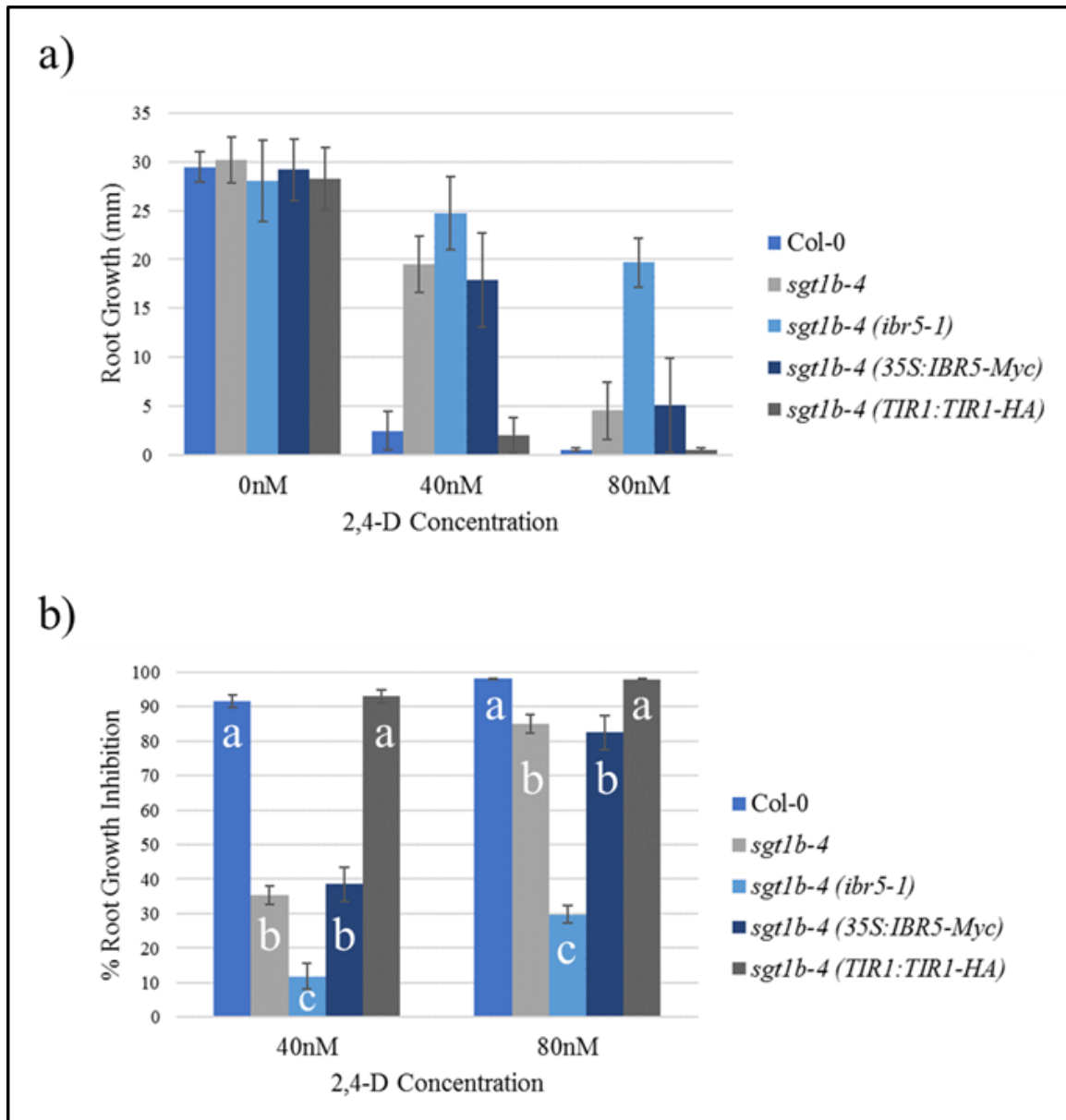


**Figure 24. *sgt1b-4* auxin resistance is rescued by overexpression of TIR1, but not *ibr5-1* or *35S:IBR5-Myc* backgrounds.** a) 4-day old seedlings were transferred to ATS media containing mock (EtOH) or indicated concentrations of 2,4-D, and new growth was measured after 4 more days. b) Percent root growth inhibition was calculated relative to mock treatment. Error bars indicate standard error of the mean. Letters indicate significant differences in percent inhibition using one-way ANOVA ( $p < 0.01$ ). Assay was performed three times with similar results.

## IV. DISCUSSION

### **IBR5 may interact directly with SCF<sup>TIR1/AFBs</sup> *in planta***

Prior to this study, two independent groups identified an interaction between IBR5 and ASK1 proteins in yeast two-hybrid screens (Risseuw et al. 2003; *Arabidopsis* Interactome Mapping Consortium 2011). If true, the interaction between IBR5 and ASK1 would help explain how IBR5 regulates Aux/IAA degradation. While these proteins were observed to interact *in vitro* using GST pulldown (Fig. 3a,b), the interaction was not observed when tested *in vivo* with Co-IPs (Fig. 4). The negative result from Co-IP assays does not necessarily mean that these two proteins are not interacting inside live plant cells, as there may be particular physiological conditions which favor the interaction, such as subcellular localization or local auxin concentration, or there may be technical conditions not properly met for the assay to show a positive result. For that reason, it may be helpful to try other protein-protein interaction assays *in planta* such as bi-molecular fluorescence complementation (BiFC) or split-luciferase complementation assay (SLCA). In these assays, proteins of interest are fused with either N- or C- terminal portions of a fluorescent protein, expressed in plant cells, and complementary fluorescent fragments fluoresce only when brought closely together, indicating that the proteins of interest are interacting with each other. These assays are superior in many ways to Co-IP, including that they are observed inside living plant cells, they provide subcellular localization of interactions, and can be subjected to different conditions to study the basis of an interaction.

ASK1 is a core component of a variety of SCF complexes with different F-box proteins (Dezfulian et al. 2012). This raises the possibility that proteins interacting with ASK1 are either part of an SCF complex or are indirectly interacting with ASK1 as a substrate for an SCF complex, such as Aux/IAAs interact with SCF<sup>TIR1/AFBs</sup>. Our lab has previously shown that IBR5 is degraded by the 26S proteasome, since treatment with MG132 stabilized IBR5 protein (Katti, unpublished). However, it is unclear how, or under what circumstances IBR5 is targeted for degradation.

ASK1 has been identified in multiple large-scale phosphorylation site analyses as a putative phosphoprotein, with a serine (S79) residue as the phosphosite (Sugiyama et al. 2008; Nakagami et al. 2010; Umezawa et al. 2013; Roitinger et al. 2015; Bhaskara et al. 2017). This is consistent with IBR5 being a putative dual-specificity phosphatase, since proteins containing the conserved dual-specificity phosphatase active-site motif are shown capable of desphosphorylating tyrosine or serine/threonine residues (Keyse 1995; Camps, Nichols, and Arkinstall 2000). In the case that IBR5 truly interacts with ASK1 *in planta*, the effect of IBR5 on the phosphorylation status of ASK1 and the components of the SCF<sup>TIR1AFBs</sup> complex should be investigated.

### **IBR5 affects TIR1 and ASK1 protein levels**

Given that *ibr5* mutants display auxin response defects, especially the enhancement of Aux/IAA degradation, ways in which IBR5 may be involved in regulating SCF<sup>TIR1</sup> were explored. If IBR5 and ASK1 interact in plant cells, this may help explain how IBR5 regulates Aux/IAA degradation and auxin-responsive gene induction. Cullin-RING ligases (CRLs), including SCF complexes, are shown to be tightly regulated

by post-translational modifications that cycle complex components depending upon cellular environment (Reitsma et al. 2017). In addition, the components of SCF<sup>TIR1</sup>, CUL1, ASK1, and TIR1, are shown to be degraded via the 26S proteasome (Stuttman et al. 2009) (Fig. 5a,b) (Fig. 11a). It was found that the three *ibr5* mutant alleles tested, as well as *35S:IBR5-Myc*, show an increased level of ASK1 protein relative to Col-0 (Fig. 6a,b). Further experiments showed that TIR1 protein levels are also elevated in *ibr5* mutants and *35S:IBR5-Myc* (Fig. 6c,d). Worth noting is that TIR1 protein levels were only elevated in *35S:IBR5-Myc* shoot tissue, but only barely elevated, if at all, in root tissue. qPCR analysis confirmed that transcript levels of *ASK1* (Fig. 9) and *TIR1* (Fig. 8a,b) are not elevated in *ibr5* mutants and *35S:IBR5-Myc*. These results suggest IBR5 affects the abundance of SCF<sup>TIR1</sup> subunits at the post-translational level. Alternatively, the physical translation of these proteins may be altered in *ibr5* mutants after transcription, however this hypothesis was not tested in this study.

If IBR5 regulates TIR1 and ASK1, it may regulate other F-box proteins similarly. Jasmonic acid (JA) signaling involves the activity of SCF<sup>COI1</sup> (Xu et al. 2002), and the F-box protein *CORONATINE-INSENSITIVE1 (COI1)* is 34% identical in nucleotide sequence to *TIR1* (Ruegger et al. 1998). COI1 could also be regulated by IBR5, however this is unlikely given that *ibr5* mutants show no altered response to MeJA, indicating IBR5 is not involved in JA signaling (Fig. 7a,b). If a physical interaction between ASK1 and IBR5 underlies the regulation of auxin signaling by IBR5, it would be worth testing if any other F-box proteins besides TIR1 and COI1 are affected by IBR5.

## Post-translational regulation of TIR1 appears unaffected by IBR5

Since the SCF<sup>TIR1</sup> complex gains specificity to the auxin pathway through the co-receptor TIR1, I focused on studying how IBR5 regulates TIR1 to modulate auxin responses. It has been demonstrated that TIR1 is regulated in many ways to fine-tune auxin signaling. miR393 is a stress-induced microRNA that targets mRNAs of the *TIR1/AFBs* family, downregulating their expression (Navarro et al. 2006; Si-Ammour et al. 2011; Chen, Li, and Xiong 2012). However, IBR5 appears uninvolved with miR393 since TIR1 transcription is only minorly decreased by altering IBR5 (Fig. 8a,b), and the expected result would be a correlated decrease, not increase of TIR1 protein (Fig. 6c,d).

TIR1 protein levels in *ibr5-1* and *35S:IBR5-Myc* lines remained higher than in Col-0 when seedlings were treated with MG132 (Fig. 11a), suggesting that TIR1 protein levels in these backgrounds are not elevated due to decreased 26S proteasomal degradation. Further, *in vitro* degradation of TIR1 was tested in *ibr5-1* and *35S:IBR5-Myc* with an equalized beginning amount of TIR1-HA protein, and no difference in degradation was observed relative to Col-0 (Fig. 11b). Although this supports that the 26S proteasome is typically degrading TIR1 in *ibr5-1* and *35S:IBR5-Myc* backgrounds, it could still be possible that the 26S proteasomal pathway is altered by an unknown mechanism to modulate the steady-state levels of TIR1. The subcellular localization of TIR1 and/or the 26S proteasome, for example, could alter the steady-state levels of TIR1 *in vivo* without affecting TIR1 stability *in vitro*.

## **Regulation of the auxin pathway by IBR5 is partially independent of HSP90 and SGT1b**

In *Arabidopsis*, heat stress (30°C) results in the stabilization of TIR1 protein *in vivo* in as little as 1-2hrs, and this stabilization is dependent upon the chaperone protein HSP90 and its co-chaperone SGT1b (Wang et al. 2016). Results presented in this study showed that *ibr5-1* and *35S:IBR5-Myc* seedlings had an increase in TIR1 stabilization in response to heat stress, as was the case with Col-0 (Fig. 12a). Heat stress also mediates the physiological effect of hypocotyl elongation through an increase in auxin biosynthesis, resulting in increased cell expansion (Franklin et al. 2011). Despite heat stress-induced TIR1 stabilization being unaffected, heat stress-induced hypocotyl elongation was seen to be diminished in *ibr5* mutants (Fig. 14a). Given that *ibr5* mutants are resistant to auxin (Zolman et al. 2000; Monroe-Augustus, Zolman, and Bartel 2003; Strader, Monroe-Augustus, Bartel 2008; Jayaweera et al. 2014), it makes sense that they are also defective in a physiological response that is partially dependent upon an increase in auxin biosynthesis. An unexpected result was that *ibr5-4* seedlings experienced root growth inhibition at 30°C (Fig. 14b). The fact that *ibr5-4* was the only *ibr5* allele to show this phenotype suggests this is due to the decreased phosphatase activity, and since a mutated protein is actually present in this line, there may be a dominant negative effect occurring due to the decreased phosphatase activity. Alternatively, there may be off-target mutations in the *ibr5-4* line that were not removed with the backcrossing performed by Jayaweera et al. (2014). Testing if an *ibr5-4* line complemented with a functional version of IBR5 recovers this phenotype would help confirm this phenotype is due to the *ibr5-4* mutation.

IBR5 acts together with HSP90 and SGT1b in the disease resistance pathway to stabilize R-proteins (Liu et al. 2015). Interestingly, IBR5 and HSP90-SGT1b have opposite effects on the steady-state levels of TIR1 (Fig. 6c,d; Wang et al. 2015). It appears that HSP90-SGT1b-mediated stabilization of TIR1 is independent of IBR5 for the following reasons. Using crystal structure analysis, the chemical GDA is demonstrated to inhibit HSP90 activity by fitting inside a pocket that is understood to be responsible for substrate interactions (Stebbins et al. 1997). GDA treated plants show a reduction in TIR1 protein levels, and this same effect was observed in *ibr5-1* and *35S:IBR5-Myc* plants (Fig. 12c), though these lines still had relatively more TIR1 protein. GDA treatment also stabilizes *AXR3NT-GUS* in these three lines relatively similarly (Fig. 13). These findings suggest that HSP90-dependent stabilization of TIR1 does not require IBR5. Further, it could indicate that IBR5 activity in the auxin response pathway is independent of HSP90-SGT1b.

SGT1b was implicated in jasmonic acid signaling when the SGT1b mutant *eta3* (*enhancer of tir1-1 auxin resistance3*) exhibited resistance to MeJA (Gray et al. 2003). More recent findings that HSP90-SGT1b bind with TIR1 and COI1, and *sgt1b* mutants show reductions in TIR1 and COI1 protein levels (Wang et al. 2015; Zhang et al. 2015), strongly suggest that SGT1b and HSP90 are integral for normal stabilization and activity of these F-box proteins.

In this study, the genetic interaction was examined between IBR5 and SGT1b to see if these proteins work together in regulating auxin response. Double mutants between three *ibr5* alleles and *sgt1b-4* each had a slight increase in primary root growth resistance to IAA, which supports that these proteins act at least partially independent of each other

in the auxin pathway. It is curious that while *sgt1b-4* has decreased TIR1 protein levels, and *ibr5-1* and *35S:IBR5-Myc* have increased TIR1 protein levels, *ibr5-1 sgt1b-4* and *35S:IBR5-Myc sgt1b-4* double mutants did not have intermediate resistance to auxin. Furthermore, overexpression of native TIR1 did recover *sgt1b-4* sensitivity to IAA. This suggests that this overabundant TIR1 protein in *ibr5-1* and *35S:IBR5-Myc* is not functioning normally as in wild-type plants. A more complete picture of the genetic interaction between IBR5 and SGT1b will be seen by analyzing the TIR1 protein levels in double mutant lines.

### **IBR5 may regulate the localization of TIR1/ASK1**

One of the more striking results from this study was that DII-Venus is stabilized in *ibr5* mutants, and drastically stabilized in *35S:IBR5-Myc*, compared to Col-0 (Fig. 17a,b; Fig. 18a,b). This was an unexpected result, since *HS:AXR3NT-GUS* has been repeatedly shown to be rapidly degraded in *ibr5* mutants (Fig. 15a; Jayaweera et al. 2014; Strader, Monroe-Augustus, Bartel 2008), and the same is true for *IAA28:IAA28-Myc* in *ibr5* mutants (Strader, Monroe-Augustus, Bartel 2008). When comparing these three different Aux/IAA reporter constructs, DII-Venus is the only one with an added nuclear localization signal (NLS) (Brunoud et al. 2012). Aux/IAs possess two conserved NLS sequences that span between domains I & II (Abel, Oeller, and Theologis 1994; Wu et al. 2012). While it can be assumed that AXR3NT-GUS is localized to the nucleus, as it consists of IAA17 domains I & II, Gray et al. (2001) noted that it is primarily nuclear localized, implying some GUS expression was observed outside of the nucleus. In addition, our own lab has observed that IAA28-GUS is localized both to the nucleus and

cytoplasm of cells (Karunaratne, unpublished). In any case, the variation in the conserved domains of Aux/IAAs are known to differentially regulate their stability (Abel, Oeller, and Theologis 1994; Dreher et al. 2006; Ludwig et al. 2014). The incongruent stabilization of Aux/IAA reporters in *ibr5* mutant backgrounds could be explained by the variation in domains present, leading to differential SCF<sup>TIR1/AFBs</sup> binding (domain II) or subcellular localization (domain I/II).

DII-Venus is arguably a better system to use in determining Aux/IAA steady state levels, since it does not require induction by heat-shock and is driven by a constitutive promoter. It is also worth noting that heat stress is well-established to regulate the auxin pathway (Franklin et al. 2011; Wang et al. 2016), which could confound results observed with the *HS:AXR3NT-GUS* reporter construct. If one is to accept that DII-Venus is stabilized in *ibr5* mutants, then it must be that there is a fundamental difference between DII-Venus and AXR3NT-GUS.

TIR1/AFBs are necessary for reception of auxin (Dharmasiri et al. 2015), thus the abundance of TIR1 protein correlates with a plant's ability to respond to the cellular signal of auxin. Indeed, researchers have found that the overexpression of TIR1 results in hypersensitivity to auxin, even at normal physiological levels of IAA, causing inhibition of root growth (Gray et al. 1999). *ibr5* mutants and *35S:IBR5-Myc* lines have increased TIR1 levels, yet *ibr5* mutants are resistant to auxin, and *35S:IBR5-Myc* has wild-type sensitivity to auxin. The best explanation for this is that the TIR1 protein in these lines is not achieving its normal function in auxin response. While an overabundance of functional TIR1 in *ibr5* could explain the rapid degradation of AXR3NT-GUS, this does not explain the stabilization of DII-Venus. IBR5 could impact the folding and/or

subcellular localization of TIR1 to regulate auxin response. TIR1 that is not localized in the nucleus could be prevented from binding with its Aux/IAA substrates to mediate their ubiquitination and 26S proteasomal degradation. DII-Venus could possibly localize to the nucleus to a greater extent than AXR3NT-GUS due to its smaller size and second inserted NLS, and AXR3NT-GUS could be degraded in *ibr5* mutants more efficiently due to accumulated cytoplasmic SCF<sup>TIR1/AFBs</sup> and associated degradation machinery. In eukaryotes the 26S proteasome can indeed be found both in nuclei and cytoplasm to serve common and specific functions (Peters, Franke, and Kleinschmidt 1994).

Interestingly, substitutions at TIR1 E12 and E15 residues, which affect its binding to an SCF through CUL1, actually stabilize TIR1 while simultaneously decreasing auxin response (Yu et al. 2015). This finding could mean that the 26S proteasomal degradation of TIR1, and possibly ASK1, is a result of autocatalytic degradation, a process known in yeast and animals, where an F-box protein is ubiquitinated by the SCF complex with which it is bound (Schmidt et al. 2009; Luke-Glaser et al. 2007; Galan and Peter 1999). If TIR1 nuclear localization is being altered in *ibr5* mutants, the lack of assembly into nuclear SCF complexes and associated autocatalytic degradation would explain TIR1 stabilization in *ibr5* mutants. This is also consistent with the fact that IBR5 does not alter *in vitro* degradation of TIR1 (Fig. 11b), as the effects of nuclear localization are negated in a cell-free system.

TIR1 is typically localized in the nucleus, where it assembles into SCF<sup>TIR1</sup> and interacts with the HSP90-SGT1b chaperone module (Dezfulian et al. 2016; Wang et al. 2016). In the brassinosteroid (BR) signaling pathway, HSP90 has been implicated in sustaining the nuclear localization of BIN2, a protein kinase involved in BR signaling

(Samakovli et al. 2014). This article also illustrated that GDA treatment causes HSP90 translocation into the cytoplasm, bringing BIN2 along with it, and possibly other HSP90 client proteins. A more recent article from Watanabe et al. (2016) demonstrated that TIR1 localization is heavily shifted from the nucleus to the cytoplasm when plants are treated with the chemical radicicol, an HSP90 inhibitor similar to GDA. Thus, HSP90 is likely responsible for localizing TIR1 to the nucleus. Why the treatment of plants with GDA results in TIR1 destabilization is unclear, though it could conceivably be due to loss of chaperone activity of HSP90-SGT1b, separately from its localizing effects.

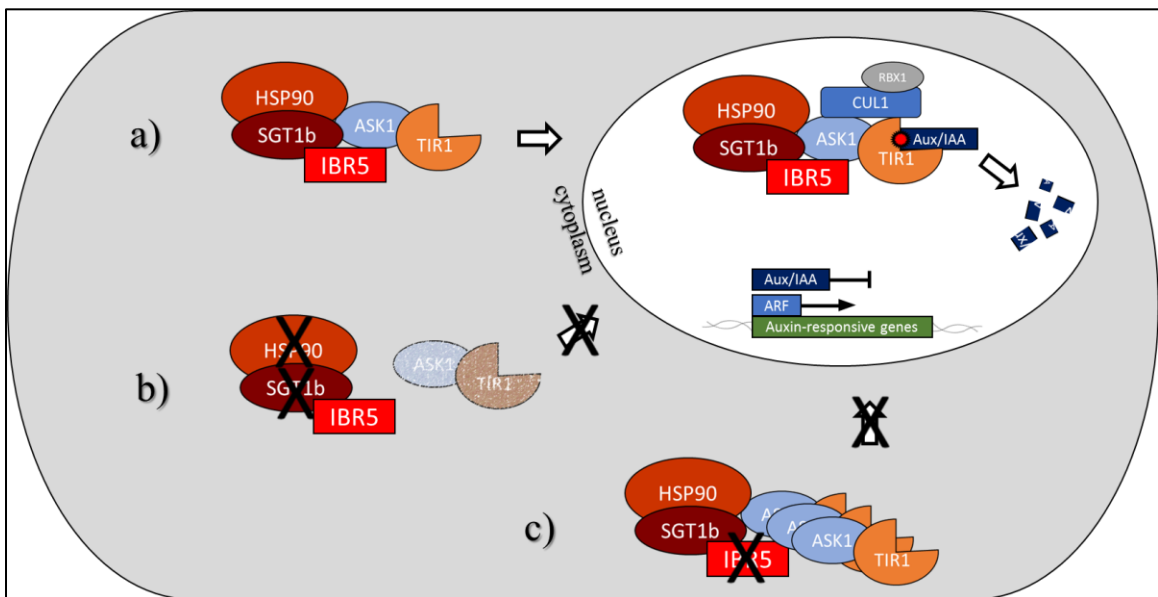


**Figure 25. Hypothetical model of IBR5 regulating TIR1/ASK1 subcellular localization via the HSP90-SGT1b chaperone module.** a) Under normal conditions, the TIR1/ASK1 substrate recognition module is properly folded and localized to the nucleus via a complex of IBR5-HSP90-SGT1b. TIR1/ASK1 in the nucleus assembles into SCF<sup>TIR1</sup> and contributes to Aux/IAA ubiquitination and subsequent degradation by the 26S proteasome. b) When HSP90-SGT1b activity is inhibited by GDA, radicicol, or by genetic alteration, TIR1/ASK1 are destabilized and will remain significantly in the cytoplasm, and auxin responses are defective. c) When IBR5 is mutated, HSP90-SGT1b chaperone capabilities remain intact, while TIR1/ASK1 nuclear localization is diminished. This results in accumulation of TIR1/ASK1 in the cytoplasm, leading to defects in auxin response.

## Conclusion and Further Directions

The results shown in this study strongly support a role for IBR5 in regulating auxin response by controlling TIR1 nuclear localization (Fig. 25). Further experiment must be done to confirm this hypothesis, including localization studies of TIR1 and ASK1 in *ibr5* mutants. The HSP90-SGT1b chaperone module is necessary for proper TIR1 stabilization, as well as TIR1 nuclear localization. These two functions of HSP90-SGT1b appear to be separate processes, and both help to fine-tune the auxin signaling pathway. IBR5 is known to form a complex with HSP90-SGT1b to stabilize R-proteins in disease resistance (Liu et al. 2015), and there is some evidence to show that IBR5 also interacts with the SCF<sup>TIR1/AFBs</sup> complex through ASK1, though this needs to be confirmed with alternative *in vivo* methods. Additionally, the exact way in which a putative IBR5-HSP90-SGT1b interacts with the SCF<sup>TIR1/AFBs</sup> complex needs to be examined further. Together, the results in this study suggest that IBR5 is not involved with the HSP90-mediated stabilization of TIR1, but it does appear IBR5 is necessary for HSP90-mediated nuclear localization of TIR1. The mechanism by which IBR5 may promote the nuclear localization of TIR1 remains unclear. It is likely that IBR5 dephosphorylates its interacting proteins to modulate their activity. In this case, dephosphorylation of HSP90-SGT1b, or possibly ASK1, may be a key factor in the regulation of auxin signaling by IBR5.

## REFERENCES

- Abel, S., Oeller, P. W., Theologis, A. (1994) Early auxin-induced genes encode short-lived nuclear proteins. *Proc Natl Acad Sci (91)*, 326-330.
- Arabidopsis* Interactome Mapping Consortium (2011) Evidence for Network Evolution in an *Arabidopsis* Interactome Map. *Science 333(6042)*, 601-607.
- Azevedo, C., Betsuyaku, S., Peart, J., Takahashi, A., Noël, L., Sadanandom, A., Casais, S., Parker, J., Shirasu, K. (2006) Role of SGT1 in resistance protein accumulation in plant immunity. *The EMBO Journal 25(9)*, 2007-2016.
- Bansal, P. K., Abdulle, A., Kitigawa, K. (2004) Sgt1 Associates with HSP90: and Initial Step of Assembly of the Core Kinetochore Complex. *J Mol Cell Biol 24(18)*, 8069-8079.
- Bhaskara, G. B., Wen, T. N., Nguyen, T. T., Verslues, P. E. (2017) Protein phosphatase 2Cs and *Microtubule-Associated Stress Protein 1* control microtubule stability, plant growth, and drought response. *The Plant Cell 29(1)*, 169-191.
- Brunoud, G., Wells, D. M., Oliva, M., Larrieu, A., Mirabet, V., Burrow, A. H., Beeckman, T., Kepinski, S., Traas, J., Bennett, M. J., Vernoux, T. (2012) A novel sensor to map auxin response and distribution at high spatio-temporal resolution. *Nature (482)*, 103-106.
- Camps, M., Nichols, A., Arkinstall, S. (2000) Dual specificity phosphatases: a gene family for control of MAP kinase function. *FASEB J 14(1)*, 6-16.

- Catlett, M. G., Kaplan, K. B. (2006). Sgt1p is a unique co-chaperone that acts as a client adaptor to link HSP90 to Skp1p. *J Biol Chem* 281(44), 33739-33748.
- Chen, B., Zhong, D., Monteiro, A. (2006) Comparative genomics and evolution of the HSP90 family of genes across all kingdoms of organisms. *BMC Genomics* 7(156).
- Chen, H., Li, Z., Xiong, L. (2012) A plant microRNA regulates the adaptation of roots to drought stress. *FEBS Letters* 586(12), 1742-1747.
- Choi, C. M., Gray, W. M., Mooney, S., Hellmann, H. (2014) Composition, Roles, and Regulation of Cullin-based Ubiquitin E3 Ligases. *The Arabidopsis Book*.
- Chen, Z., Bao, M., Sun, Y., Yang, J., Xu, X., Wang, J., Han, N., Bian, H., Zhu, M. (2011) Regulation of auxin response by miR393-targeted *transport inhibitor response protein 1* is involved in normal development in *Arabidopsis*. *Plant Mol Biol* 77(6), 619-629.
- Dezfulian, M. H., Jalili, E., Roberto, D. K. A., Moss, B. L., Khoo, K., Nemhauser, J. L., Crosby, W. L. (2016) Oligomerization of SCF<sup>TIR1</sup> is essential for Aux/IAA degradation and auxin signaling in *Arabidopsis*. *PLoS Genet* 12(9), e1006301.
- Dezfulian, M. H., Soulliere, D. M., Dhaliwal, R. K., Sareen, M., Crosby, W. L. (2012) The *SKP1-Like* gene family of *Arabidopsis* exhibits a high degree of differential gene expression and gene product interaction during development. *PLoS ONE* 7(11). e50984.
- Dharmasiri, N., Dharmasiri, S., & Estelle, M. (2005). The F-box protein TIR1 is an auxin receptor. *Nature* (435), 441-445.

- Dharmasiri, N., Dharmasiri, S., Weijers, D., Lechner, E., Yamada, M., Hobbie, L., Ehrismann, J. S., Jürgens, G., Estelle, M. (2005) Plant development is regulated by a family of auxin receptor f-box proteins. *Dev Cell* 9(1), 109-119.
- Dreher, K. A., Brown, J., Saw, R. E., Callis, J. (2006) The *Arabidopsis* Aux/IAA protein family has diversified in degradation and auxin responsiveness. *The Plant Cell* (18), 699-714.
- Farrás, R., Ferrando, A., Jásik, J., Kleinow, T., Ökrész, L., Tiburcio, A., Salchert, K., del Pozo, C., Schell, J., Koncz, C. (2001). SKP1-SnRK protein kinase interactions mediate proteasomal binding of a plant SCF ubiquitin ligase. *The EMBO Journal* 20(11), 2742-2756.
- Franklin, K. A., Lee, S. H., Patel, D., Kumar, S. V., Spartz, A. K., Gu, C., Ye, S., Yu, P., Breen, G., Cohen, J. D., Wigge, P. A., Gray, W. M. (2011) PHYTOCHROME-INTERACTING FACTOR 4 (PIF4) regulates auxin biosynthesis at high temperature. *Proc Natl Acad Sci* 108(50), 20231-20235.
- Friml, J., Wiśniewska, J., Benková, E., Mendgen, K., Palme, K. (2002) Lateral relocation of auxin efflux regulator PIN3 mediates tropism in *Arabidopsis*. *Nature* (415), 806-809.
- Galan, J., Peter, M. (1999) Ubiquitin-dependent degradation of multiple F-box proteins by an autocatalytic mechanism. *Proc Natl Acad Sci* 96(16), 9124-9129.

- Gray, W. M., del Pozo, J. C., Walker, L., Hobbie, L., Risseuw, E., Banks, T., Crosby, W. L., Yang, M., Ma. H., Estelle, M. (1999) Identification of an SCF ubiquitin-ligase complex required for auxin response in *Arabidopsis thaliana*. *Genes Dev* 13(13), 1678-1691.
- Gray, W. M., Hellman, H., Dharmasiri, S., Estelle, M. (2002) Role of the *Arabidopsis* RING-H2 protein RBX1 in RUB modification and SCF function. *The Plant Cell* 14(9), 2137-2144.
- Gray, W. M., Kepinski, S., Rouse, D., Leyser, O., Estelle, M. (2001) Auxin regulates SCF<sup>TIR1</sup>-dependent degradation of AUX/IAA proteins. *Nature* (414), 271-276.
- Gray, W. M., Muskett, P. R., Chuang, H., Parker, J. E. (2003) *Arabidopsis* SGT1b is Required for SCF<sup>TIR1</sup>-Mediated Auxin Response. *The Plant Cell* (15), 1310-1319.
- Gray, W. M., Östin, A. Sandberg, G., Romano, C. P., Estelle, M. (1998). High temperature promotes auxin-mediated hypocotyl elongation in *Arabidopsis*. *Proc Natl Acad Sci* 95(12), 7197-7202.
- Hagen, G., Guilfoyle, T. (2002) Auxin-responsive gene expression: genes, promoters and regulatory factors. *Plant Mol Biol* (49), 373-385.
- Jakobson, L., Vaahtera, L., Nuhkat, M., Wang, C., Wang, Y., Hörak, H., Valk, E., Pechter, P., Sindarovska, Y., Tang, J., Xiao, C., Xu, Y., Talas, U. G., Garcia-Sosa, A. T., Kangasjärvi, S., Maran, U., Remm, M., Roelfsema, M. R. G., Hu, H., Kangasjärvi, J., Loog, M., Schroeder, J. I., Kollist, H., Brosché. (2016) Natural variation in *Arabidopsis* Cvi-0 accession reveals important role of MPK12 in guard cell CO<sub>2</sub> signaling. *PLoS Biol* 14(12), e2000322.

- Jammes, F., Song, C., Shin, D., Munemasa, S., Takeda, K., Gu, D., Cho, D., Lee, S., Giordo, R., Sritubtim, S., Leonhardt, N., Ellis, B. E., Murata, Y., Kwak, J. M. (2009) Map kinases MPK9 and MPK12 are preferentially expressed in guard cells and positively regulate ROS-mediated ABA signaling. *Proc Natl Acad Sci* *106(48)*, 20520-20525.
- Jayaweera, T., Siriwardana, C., Dharmasiri, S., Quint, M., Gray, W. M., & Dharmasiri, N. (2014). Alternative Splicing of Arabidopsis IBR5 Pre-mRNA Generates Two IBR5 Isoforms with Distinct and Overlapping Functions. *PLoS ONE* *9(8)*. e102301.
- Jefferson, A. (1987) Assaying chimeric genes in plants: The GUS gene fusion system. *Plant Mol Biol Rep* *5(4)*, 387-405.
- Johnson, K. L., Ramm, S., Kappel, C., Ward, S., Leyser, O., Sakamoto, T., et al. (2015) The Tinkerbelle (Tink) Mutation Identifies the Dual-Specificity MAPK Phosphatase INDOLE-3-BUTYRIC ACIDRESPONSE5 (IBR5) as a Novel Regulator of Organ Size in Arabidopsis. *PLoS ONE* *10(7)*: e0131103.
- Keyse, S. M. (1995) An emerging family of dual specificity MAP kinase phosphatases. *Biochim Biophys Acta* (*1265*), 152-160.
- Kitigawa, K., Skowyra, D., Elledge, S. J., Harper, W., Hieter, P. (1999). SGT1 Encodes an Essential Component of the Yeast Kinetochores Assembly Pathway and a Novel Subunit of the SCF Ubiquitin Ligase Complex. *Molecular Cell* (*4*), 21-33.

- Krogan, N. T., Hogan, K., Long, J. A. (2012) APETALA2 negatively regulates multiple floral organ identity genes in *Arabidopsis* by recruiting the co-repressor TOPLESS and the histone deacetylase HDA19. *Development* 139(22), 4180-4190.
- Lee, J. S., Wang, S., Sritubtim, S., Chen, J. G. Ellis, B. E. (2009) *Arabidopsis* mitogen-activated protein kinase MPK12 interacts with the MAPK phosphatase IBR5 and regulates auxin signaling. *The Plant Journal* (57), 975-985.
- Li, H., Tiwari, S. B., Hagen, G., Guilfoyle, T. J. (2011) Identical amino acid substitutions in the repression domain of auxin/indole-3-acetic acid proteins have contrasting effects on auxin signaling. *Plant Physiology* 155(3), 1252-1263.
- Li, S., Xie, Z., Hu, C., Zhang, J. (2016) A review of auxin response factors (ARFs) in plants. *Front Plant Sci* 7(47).
- Liu, J., Yang, H., Bao, F., Ao, K., Zhang, X., Zhang, Y., & Yang, S. (2015). IBR5 Modulates Temperature-Dependent, R Protein CHS3-Mediated Defense Responses in Arabidopsis. *PLoS ONE Genetics* 11(0), e1005584.
- Livak, K. J., Schmittgen, T. D. (2001) Analysis of relative gene expression data using real-time quantitative PCR and the  $2^{-\Delta\Delta C_T}$  method. *Methods* (25), 402-408.
- Ludwig, Y., Berendzen, K. W., Xu, C., Piepho, H., Hochholdinger, F. (2014) Diversity of stability, localization, interaction and control of downstream gene activity in the maize Aux/IAA protein family. *PLoS ONE* 9(9), e107346.

- Luke-Glaser, S., Roy, M., Larsen, B., Bihan, T. L., Metalnikov, P., Tyers, M., Peter, M., Pintard, L. (2007) CIF-1, a shared subunit of the COP9/Signalosome and eukaryotic initiation factor 3 complexes, regulates MEL-26 levels in the *Caenorhabditis elegans* embryo. *Mol Cell Biol* 27(12), 4526-4540.
- Marocco, K., Zhou, Y., Bury, E., Dieterle, M., Genschik, P., Krenz, M., Stolpe, T., Kretsch, T. (2006) Functional analysis of EID1, an F-box protein involved in phytochrome A-dependent light signal transduction. *The Plant Journal* 45(3), 423-438.
- Mockaitis, K., Estelle, M. (2008) Auxin receptors and plant development: A new signaling paradigm. *Annu Rev Cell Dev Biol* (24), 55-80.
- Monroe-Augustus, M., Zolman, B. K., & Bartel, B. (2003). IBR5, a Dual-Specificity Phosphatase-Like Protein Modulating Auxin and Abscisic Acid Responsiveness in Arabidopsis. *The Plant Cell* (15), 2979-2991.
- Nakagami, H., Sugiyama, N., Mochida, K., Daudi, A., Yoshida, Y., Toyoda, T., Tomita, M., Ishihama, Y., Shirasu, K. (2010) Large-scale comparative phosphoproteomics identifies conserved phosphorylation sites in plants. *Plant Physiology* 153(3), 1161-1174.
- Navarro, L., Dunoyer, P., Jay, F., Arnold, B., Dharmasiri, N., Estelle, M., Voinnet, O., Jones, J. D. G. (2006). A plant miRNA contributes to antibacterial resistance by repressing auxin signaling. *Science* 312(5772), 436-439.

- Oh, E., Zhu, J., Ryu, H., Hwang, I., Wang, Z. (2014) TOPLESS mediates brassinosteroid-induced transcriptional repression through interaction with BZR1. *Nature Communications* 5(4140).
- Perrot-Rechenmann, C. (2010) Cellular responses to auxin: division versus expansion. *Cold Spring Harb Perspect Biol* 2(5).
- Peters, J., Franke, W. W., Kleinschmidt, J. A. (1994) Distinct 19 S and 20 S subcomplexes of the 26 S proteasome and their distribution in the nucleus and the cytoplasm. *J Biol Chem* 269(10), 7709-7718.
- Petroski, M. D., Deshaies, R. J. (2005) Function and regulation of cullin-RING ubiquitin ligases. *Nat Rev Mol Cell Biol* 6(1), 9-20.
- Pufky J., Qiu, Y., Rao, M. V., Hurban, P., Jones, A. M. (2003). The auxin-induced transcriptome for etiolated *Arabidopsis* seedlings using a structure/function approach. *Funct Integr Genomics* 3(4), 135-143.
- Ramos, J. A., Zenser, N., Leyser, O., Callis, J. (2001) Rapid degradation of auxin/indoleacetic acid proteins requires conserved amino acids of domain II and is proteasome dependent. *The Plant Cell* (13), 2349-2360.
- Reitsma, J. M., Liu, X.,Reichermeier, K. Moradian, A., Sweredoski, M. J., Hess. S., Deshaies, R. J. (2017) Composition and regulation of the cellular repertoire of SCF ubiquitin ligases. *Cell* 171(6), 1326-1339.

- Risseeuw, E. P., Daskalchuk, T. E., Banks, T. W., Liu, E., Cotelesage, J., Hellman, H., Estelle, M., Somers, D. E., Crosby, W. L. (2003) Protein interaction analysis of SCF ubiquitin E3 ligase subunits from *Arabidopsis*. *The Plant Journal* 34(6), 753-767.
- Rogg, L. E., Lasswell, J., & Bartel, B. (2001) A Gain-of-Function Mutation in IAA28 Suppresses Lateral Root Development. *The Plant Cell* (13), 465-480.
- Roitinger, E., Hofer, M., Köcher, T., Pichler, P. Novatchkova, M., Yang, J., Schlögelhofer, O., Mechtler, K. (2015) Quantitative phosphoproteomics of the ataxia telangiectasia-mutated (ATM) and ataxia telangiectasia-mutated and rad3-related (ATR) dependent DNA damage response in *Arabidopsis thaliana*. *Mol Cell Proteomics* 14(3), 556-571.
- Ruegger, M., Dewey, E., Gray, W. M., Hobbie, L., Turner, J., Estelle, M. (1998) The TIR1 protein of *Arabidopsis* functions in auxin response and is related to human SKP2 and yeast Grr1p. *Genes Dev* 12(2), 198-207.
- Saibil, H. (2013) Chaperone machines for protein folding, unfolding and disaggregation. *Nat Rev Mol Cell Biol* (14), 630-642.
- Samakovli, D., Margaritopoulou, T., Prassinos, C., Milioni, D. (2014) Brassinosteroid nuclear signaling recruits HSP90 activity. *New Phytologist* 203(3), 743-757.
- Schmidt, M. W., McQuary, P. R., Wee, S., Hofmann, K., Wolf, D. A. (2010) F-box-directed CRL complex assembly and regulation by the CSN and CAND1. *Molecular Cell* 35(5), 586-597.

- Si-Ammour, A., Windels, D., Arn-Boulidoires, E., Kutter, C., Ailhas, J., Meins, F., Vasquez, F. (2011) miR393 and secondary siRNAs regulate expression of the TIR1/AFB2 auxin receptor clade and auxin-related development of *Arabidopsis* leaves. *Plant Physiology* 157(2), 683-691.
- Skarr, J. R., Pagan, J. K., Pagano, M. (2013) Mechanisms and function of substrate recruitment by F-box proteins. *Nat Rev Mol Cell Biol* 14(6).
- Spartz, A. K., Ren, H., Park, M. Y, Grandt, K. N., Lee, S. H., Murphy, A. S., Sussman, M. R., Overvoorde, P. J., Gray, W. M. (2014) SAUR inhibition of PP2C-D phosphatases activates plasma membrane H<sup>+</sup>-ATPases to promote cell expansion in *Arabidopsis*. *The Plant Cell* (26), 2129-2142.
- Stebbins, C. E., Russo, A. A., Schneider, C., Rosen, N., Hartl, F. U., Pavletich, N. P. (1997) Crystal structure of an Hsp90-geldanamycin complex: targeting of a protein chaperone by an antitumor agent. *Cell* 89(2), 239-250.
- Steensgaard, P., Garré, M., Muradore, I., Transidico, P., Nigg, E. A., Kitigawa, K., Earnshaw, W. C., Faretta, M., Musacchio, A. (2004). Sgt1 is required for human kinetochore assembly. *EMBO Rep* 5(6), 626-631.
- Strader, L. C., Chen, G. L., Bartel, B. (2010) Ethylene directs auxin to control root cell expansion. *The Plant Journal* (64), 874-884.
- Strader, L. C., Monroe-Augustus, M., & Bartel, B. (2008). The IBR5 phosphatase promotes *Arabidopsis* auxin responses through a novel mechanism distinct from TIR1-mediated repressor degradation. *BMC Plant Biology* 8(41).

- Stuttmann, J., Lechner, E., Guérois, R., Parker, J. E., Nussaume, L., Genschik, P., Noël, L. D. (2009). COP9 Signalosome- and 26S Proteasome-dependent Regulation of SCF<sup>TIR1</sup> Accumulation in *Arabidopsis*. *J Biol Chem* 284(12), 7920-7930.
- Sugiyama, N., Nakagami, H., Mochida, K., Daudi, A., Tomita, M., Shirasu, K., Ishihama, Y. (2008) Large-scale phosphorylation mapping reveals the extent of tyrosine phosphorylation in *Arabidopsis*. *Mol Syst Biol* 4(193).
- Swarup, R., Kramer, E. M., Perry, P., Knox, K., Leyser, O., Haseloff, J., Beemster, G. T. S., Bhalerao, R., Bennett, M. J. (2005) Root gravitropism requires lateral root cap and epidermal cells for transport and response to a mobile auxin signal. *Nat Cell Biol* (7), 1057-1065.
- Szemenyei, H., Hannon, M., Long, J. A. (2008) TOPLESS mediates auxin-dependent transcriptional repression during *Arabidopsis* embryogenesis. *Science* 319(5868), 1384-1386.
- Tan, X., Calderon-Villalobos, L. I. A., Sharon, M., Zheng, C., Robinson, C. V., Estelle, M., Zheng, N. (2007) Mechanism of auxin perception by the TIR1 ubiquitin ligase. *Nature* (446), 640-645.
- Tomko Jr., R. J., & Hochstrasser, M. (2013). Molecular Architecture and Assembly of the Eukaryotic Proteasome. *Annu Rev Biochem* 2013, (82).
- Tör, M., Gordon, P., Cuzick, A., Eulgem, T., Sinapidou, E., Mert-Türk, F., Can, C., Dangl, J. L., Holub, E. B. (2002) *Arabidopsis* SGT1b Is Required for Defense Signaling Conferred by Several Downy Mildew Resistance Genes. *The Plant Cell* (14), 993-1003.

- Umezawa, T., Sugiyama, N., Takahashi, F., Anderson, J. C., Ishihama, Y., Peck, S. C., Shinozaki, K. (2013) Genetics and phosphoproteomics reveal a protein phosphorylation network in the abscisic acid signaling pathway in *Arabidopsis thaliana*. *Sci Signal* 6(270).
- Walsh, T. A., Neal, R., Merlo, A. O., Honma, M., Hicks, G. R., Wolff, K., Matsumura, W., Davies, J. P. (2006) Mutations in an Auxin Receptor Homolog AFB5 and in SGT1b Confer Resistance to Synthetic Picolinate Auxins and Not to 2,4-Dichlorophenoxyacetic Acid or Indole-3-Acetic Acid in *Arabidopsis*. *Plant Physiology* (142), 542-552.
- Wang, R., Zhang, Y., Kieffer, M., Yu, H., Kepinski, S., Estelle, M. (2016) HSP90 regulates temperature-dependent seedling growth in *Arabidopsis* by stabilizing the auxin co-receptor F-box protein TIR1. *Nature Communications* 7(10269).
- Watanabe, E., Mano, S., Nomoto, M., Tada, Y., Hara-Nishimura, I., Nishimura, M., Yamada, K. (2016) HSP90 stabilizes auxin-responsive phenotypes by masking a mutation in the auxin receptor TIR1. *Plant and Cell Physiology* 57(11), 2245-2254.
- Woodward, A. W., Bartel, B. (2005) Auxin: Regulation, Action, Interaction. *Ann Bot* 95(5), 707-735.
- Wu, W., Liu, Y., Wang, Y., Li, H., Liu, J., Tan, J., He, J., Bai, J., Ma, H. (2017) Evolution analysis of the Aux/IAA gene family in plants shows dual origins and variable nuclear localization signals. *Int J Mol Sci* 18(10), 2107.

- Xu, L., Liu, F., Lechner, E., Genschik, P., Crosby, W. L., Ma, H., Peng, W., Huang, D., Xie, D. (2002) The SCF<sup>COI1</sup> ubiquitin-ligase complexes are required for jasmonate response in *Arabidopsis*. *The Plant Cell* 14(8), 1919-1935.
- Yu, H., Zhang, Y., Moss, B. L., Bargmann, B. O. R., Wang, R., Prigge, M., Nemhauser, J., & Estelle, M. (2015). Untethering the TIR1 auxin receptor from the SCF complex increases its stability and inhibits auxin response. *Nature Plants* 1(13), doi:10.1038/nplants.2014.30.
- Zhang, W., Ito, H., Quint, M., Huang, H., Noël, L. D., Gray, W. M. (2008) Genetic analysis of CAND1-CUL1 interactions in *Arabidopsis* supports a role for CAND1-mediates cycling of the SCF<sup>TIR1</sup> complex. *Proc Natl Acad Sci* 105(24), 8470-8475.
- Zhang, X., Millet, Y. A., Cheng, Z., Bush, J., Ausubel, F. M. (2015) Jasmonate signalling in *Arabidopsis* involves SGT1b-HSP70-HSP90 chaperone complexes. *Nature Plants* 1(15049), doi:10.1038/nplants.2015.49.
- Zhu, Z., Xu, F., Zhang, Y., Cheng, Y.T., Wiermer, M., Li, X., Zhang, Y. (2010) *Arabidopsis* resistance protein SNC1 activates immune responses through association with transcriptional co-repressor. *Proc Natl Acad Sci* 107(31), 13960-13965.
- Zolman, B. K., Yoder, A., Bartel, B. (2000) Genetic analysis of indole-3-butyric acid responses in *Arabidopsis thaliana* reveals four mutant classes. *Genetics* (156), 1323-1337.